

United States  
Environmental Protection  
Agency

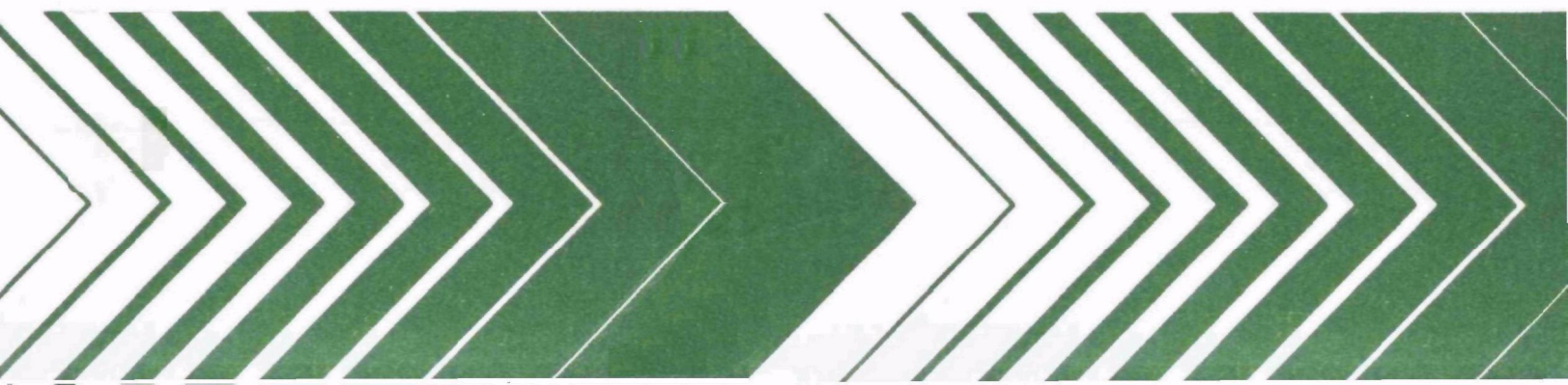
Environmental Sciences Research  
Laboratory  
Research Triangle Park NC 27711

EPA-600/3-79-020  
March 1979

Research and Development



# Reactions of Oxy Radicals in the Atmosphere



## **RESEARCH REPORTING SERIES**

Research reports of the Office of Research and Development, U.S. Environmental Protection Agency, have been grouped into nine series. These nine broad categories were established to facilitate further development and application of environmental technology. Elimination of traditional grouping was consciously planned to foster technology transfer and a maximum interface in related fields. The nine series are:

1. Environmental Health Effects Research
2. Environmental Protection Technology
3. Ecological Research
4. Environmental Monitoring
5. Socioeconomic Environmental Studies
6. Scientific and Technical Assessment Reports (STAR)
7. Interagency Energy-Environment Research and Development
8. "Special" Reports
9. Miscellaneous Reports

This report has been assigned to the ECOLOGICAL RESEARCH series. This series describes research on the effects of pollution on humans, plant and animal species, and materials. Problems are assessed for their long- and short-term influences. Investigations include formation, transport, and pathway studies to determine the fate of pollutants and their effects. This work provides the technical basis for setting standards to minimize undesirable changes in living organisms in the aquatic, terrestrial, and atmospheric environments.

This document is available to the public through the National Technical Information Service, Springfield, Virginia 22161.

EPA-600/3-79-020  
March 1979

REACTIONS OF OXY RADICALS IN THE ATMOSPHERE

by

D. G. Hendry, R. A. Kenely  
J. E. Davenport, and B. Y. Lan

SRI International  
333 Ravenswood Avenue  
Menlo Park, California 94025

Grant No. 603864

Project Officer

Marcia C. Dodge  
Atmospheric Chemistry and Physics Division  
Environmental Sciences Research Laboratory  
Research Triangle Park, North Carolina 27711

ENVIRONMENTAL SCIENCES RESEARCH LABORATORY  
OFFICE OF RESEARCH AND DEVELOPMENT  
U.S. ENVIRONMENTAL PROTECTION AGENCY  
RESEARCH TRIANGLE PARK, NORTH CAROLINA 27711

## DISCLAIMER

This report has been reviewed by the Environmental Sciences Research Laboratory, U.S. Environmental Protection Agency, and approved for publication. Approval does not signify that the contents necessarily reflect the views and policies of the U.S. Environmental Protection Agency, nor does mention of trade names or commercial products constitute endorsement or recommendation for use.

# ABSTRACT

This study has been composed of two facets: the atmospheric chemistry of peroxyacetyl nitrate (PAN) and the products of the reaction of OH with aromatic compounds which are known to be in the atmosphere.

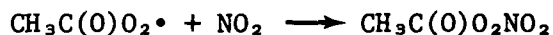
PAN dissociates rapidly in the atmosphere according to the reaction



From measurements of a temperature range of 25–39°C, the rate constant may be expressed by

$$\log k = 16.29 - 26,910/4.576T$$

The acetylperoxy radical formed can react with NO<sub>2</sub> to regenerate PAN



or react with NO



The ratio of rate constants of these two reactions,  $k_{\text{NO}}/k_{\text{NO}_2}$ , is  $3.0 \pm .7$  independent of temperature. The rate constants for reactions with NO<sub>2</sub> and NO are estimated to be  $1 \times 10^9$  and  $3 \times 10^9 \text{ M}^{-1} \text{ s}^{-1}$ , respectively.

The reactions of OH with simple aromatic hydrocarbons proceeds by two major reaction channels, abstraction of a hydrogen atom ( $k_{\text{ab}}$ ) in the benzylic position or addition of OH to the aromatic ring ( $k_{\text{ad}}$ ). For toluene, the first route primarily yields benzaldehyde, and the second route yields a mixture of cresols. The values of  $k_{\text{ab}}/(k_{\text{ab}} + k_{\text{ad}})$  for toluene, 1,4-dimethylbenzene, and 1,3,5-trimethylbenzene are  $0.15 \pm$

0.02,  $0.15 \pm 0.02$ , and  $0.02 \pm 0.006$ , respectively. Formation of m-nitrotoluene, which has been observed in some smog chamber experiments at high  $\text{NO}_2$  concentrations, results from the OH adduct reacting with  $\text{NO}_2$  and eliminating  $\text{H}_2\text{O}$ . At ambient concentrations of  $\text{NO}_2$ , this reaction is unimportant.

The reaction of OH with benzaldehyde, an important product of the toluene reaction in the atmosphere, results in an exclusive attack at the aldehydic position. Therefore, the initial stable intermediate is the benzoylperoxy radical, which can react with either NO or  $\text{NO}_2$ . Reaction of the radical with NO causes loss of  $\text{CO}_2$  and leads directly to the phenyl radical  $\text{C}_6\text{H}_5^\bullet$ . In our system, this radical produces phenol; however, in the atmosphere, it should yield ring cleavage products.

This report was submitted in fulfillment of grant number 603864 by SRI International under the partial sponsorship of the U.S. Environmental Protection Agency. This report covers a period from June 8, 1975, to June 7, 1978, and work was completed as of June 7, 1978.

## CONTENTS

ABSTRACT . . . . .	iii
FIGURES . . . . .	vi
TABLES . . . . .	vii
1. INTRODUCTION . . . . .	1
2. CONCLUSIONS AND RECOMMENDATIONS . . . . .	3
3. GAS PHASE FREE RADICAL REACTIONS OF PEROXYACETYL NITRATE .	5
Introduction . . . . .	5
Experimental Section . . . . .	6
Results and Discussion . . . . .	11
Conclusions . . . . .	34
4. GAS PHASE HYDROXYL RADICAL REACTIONS. PRODUCTS AND PATHWAYS FOR THE REACTION OF OH WITH AROMATIC HYDROCARBONS . . . . .	39
Introduction . . . . .	39
Experimental Section . . . . .	40
Results . . . . .	42
Discussion . . . . .	43
5. GAS PHASE HYDROXYL RADICAL REACTIONS. PRODUCTS AND PATHWAYS FOR THE REACTION OF OH WITH BENZALDEHYDE . . .	53
Introduction . . . . .	53
Experimental Section . . . . .	54
Results . . . . .	55
Discussion . . . . .	60
REFERENCES AND NOTES . . . . .	63

# FIGURES

Number	Page
1. U-Tube for Collection of PAN . . . . .	8
2. Fraction of PAN Remaining ( $[\text{PAN}]_t/[\text{PAN}]_0$ ) Versus Time for Decomposition of $1.72 \times 10^{-4}$ M in the Presence of $4.1 \times 10^{-4}$ M NO at 25°C . . . . .	17
3. $\ln(k_{\text{obs}}^{\text{NO}})$ Versus $1/T$ ( $\text{K}^{-1}$ ) for Decomposition of PAN in the Presence of NO . . . . .	20
4. Observed First-Order Rate Constants, $k_{\text{obs}}^{\text{RCHO}}$ for Decomposition of PAN at 25°C in the Presence of: $\text{CH}_3\text{CHO}$ With and Without Added $\text{O}_2$ ; and $\text{C}_2\text{H}_5\text{CHO}$ With and Without Added $\text{O}_2$ . . . . .	21
5. Observed First-Order Rate Constants, $k_{\text{obs}}^{\text{CHCl}_3}$ , for the Decomposition of PAN at 55°C in $\text{CHCl}_3/\text{CCl}_4$ Solutions . . . . .	24
6. Observed Rate Constant, $k_{\text{obs}}^{\text{NO}_2}$ , Versus $[\text{NO}_2]$ for Decomposition of PAN in the Presence of Added $\text{NO}_2$ at: 25°C, Slope = $(0.064 \pm 0.015) \times 10^{-4} \text{ M}^{-1} \text{ s}^{-1}$ ; Intercept = $(0.015 \pm 0.05) \times 10^{-4} \text{ s}^{-1}$ ; 34.3°C, Slope = $(0.21 \pm 0.04) \times 10^{-4} \text{ M}^{-1} \text{ s}^{-1}$ ; Intercept = $(0.045 \pm 0.15) \times 10^{-4} \text{ s}^{-1}$ ; and 43.9°C, Slope = $(0.55 \pm 0.07) \times 10^{-4} \text{ M}^{-1} \text{ s}^{-1}$ ; Intercept = $(0.030 \pm 0.4) \times 10^{-4} \text{ s}^{-1}$ . . . . .	26
7. Concentration of $\text{NO}_2^*$ (o - o), PAN + PAN $^*$ (● - ●), PAN (▲ - ▲), and PAN $^*$ (◊ - ◊) Versus Time for Decomposition of $0.78 \times 10^{-4}$ M PAN in the Presence of $3.15 \times 10^{-4}$ M $^{15}\text{NO}_2$ at 25°C . . . . .	28
8. Reciprocal Corrected Rate Constant $(k_{\text{obs}}^{\text{NO}_x} - k_{\text{obs}}^{\text{NO}_2})^{-1}$ Versus $[\text{NO}_2]/[\text{NO}]$ for Decomposition of PAN in the Presence of Added $\text{NO}_2$ and NO at: 25°C, 34.3°C, 39.0°C, and 43.9°C . . . . .	36



## TABLES

<u>Number</u>	<u>Page</u>
1. Observed Rate Constants ( $k_{\text{obs}}$ ) for PAN Decompositions in the Absence of Added Reactants at Various Temperatures . . . . .	9
2. Observed First-Order Rate Constants, $k_{\text{obs}}^{\text{NO}}$ for Decomposition of PAN in the Presence of NO at Various Temperatures . . . . .	18
3. Selected Infrared Absorption Frequencies ( $\nu$ ) for PAN, $^{15}\text{N}$ -Labelled PAN, $\text{NO}_2$ , and $^{15}\text{NO}_2$ . . . . .	29
4. Kinetic Parameters for Decomposition of $0.78 \times 10^{-4}$ M PAN in the Presence of $3.15 \times 10^{-4}$ M $^{15}\text{NO}$ , at $25^\circ\text{C}$ . . . . .	30
5. Rate Constants and Reaction Conditions for Decomposition of PAN in the Presence of Added NO and $\text{NO}_2$ at Various Temperatures . . . . .	35
6. Least Squares Data for Figure 8 and Calculated Values of $k_2/k_1$ for Decomposition of PAN in the Presence of Added $\text{NO}_2$ and NO at Various Temperatures . . . . .	37
7. Distribution of Individual Products as a Function of $[\text{NO}_2]$ Added for Reaction of OH With Toluene Plus $9.7 \times 10^{16}$ Molec $\text{cm}^{-3}$ $\text{O}_2$ . . . . .	45
8. Distribution of Individual Products as a Function of $[\text{O}_2]$ Added and of the Total Pressure for Reaction of OH with Toluene Using $1.39 \times 10^{14}$ Molec $\text{cm}^{-3}$ Added $\text{NO}_2$ . . . . .	45
9. Products and Rate Constant Ratios $[k_1/(k_1 + k_2)]$ for Reactions of OH With Various Hydrocarbons in the Presence of $\text{NO}_2$ and $\text{O}_2$ . . . . .	46
10. Reactivity and Positional Selectivity of Ring-Addition to Toluene by Various Species . . . . .	49
11. Calculated Values of 3-Nitrotoluene ( $3\text{-NO}_2\text{C}_6\text{H}_4\text{CH}_3$ /Total Products) from OH-Toluene Reaction as a Function of $\text{NO}_2$ Concentration . . . . .	52
12. Atmospheric Products for the Reactions of Aromatic Hydrocarbons with OH . . . . .	52
13. Percent Yield of Phenol ( $100 \times \text{PhOH}/\text{PhCHO}$ ) as a Function of Added $\text{NO}_2$ , $\text{O}_2$ and Total Pressure . . . . .	56

# TABLES (Cont.)

	<u>Page</u>
14. Wall and Gas Phase Products of the OH-PhCHO Reaction as a Function of Added NO <sub>2</sub> . . . . .	57
15. Field Ionization Mass Spectral Analysis of Wall Residue for OH-PhCHO Reaction . . . . .	58

## 1. INTRODUCTION

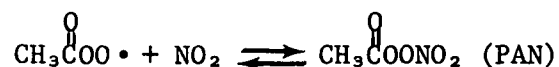
Our understanding of the atmospheric phenomenon of photochemical smog has evolved gradually since the late 1930s, when an air pollution problem was recognized in the Los Angeles air basin. The development of our knowledge can be broken down into three distinct phases. In the first phase, up to the mid-1950s, a qualitative understanding was established on how the interaction of hydrocarbons and  $\text{NO}_x$  with sunlight led to smog formation, and what some of the effects of smog on the environment were.

During the next 15 years (about 1955-1970), research centered on identifying many of the basic characteristics of smog, including the  $\text{NO}_x$ - $\text{O}_3$ -sunlight equilibrium, hydrocarbon structural effects on ozone formation and eye irritation, and major intermediates contributing to the effects associated with the overall process.

Finally, since about 1970, we have worked to understand the chemistry of smog formation at a molecular level. The key concept has been the realization of the dominant role of OH radical in reactions of hydrocarbons. The key tool has been the computer, which has allowed us to combine information on individual reactions to determine whether the overall concentrations of observed intermediates could be accurately simulated. Kinetic data, which are absolutely necessary for the computer calculations, were determined for many of the reactions during this time. Using computer simulation, it is now possible to determine which reactions are the most crucial and to subject them to further study. Thus, the research effort can now be limited to the most crucial areas, which should lead to an accurate description of photochemical smog formation that can be used to reliably predict formation of intermediates such as  $\text{NO}_2$ , PAN, and ozone under environmental conditions.

The work reported here considers two important aspects of photochemical smog, both of which are essential to a quantitative understanding

of the chemistry of the atmosphere. The first is the chemistry of peroxyacetyl nitrate (PAN), a compound that was identified in the Los Angeles atmosphere in early studies. We show that this compound is not a chemically inert species, as had been thought, but one that can have a significant effect on the overall chemistry of smog because it exists in equilibrium with the radical intermediates from which it is formed.

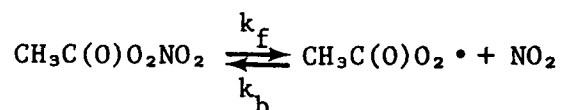


Thus PAN can act as a radical sink or source, depending on the concentrations of the peroxyacetyl radical and  $\text{NO}_2$  in the atmosphere, and can thereby have a large effect on the atmospheric chemistry.

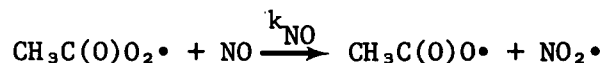
The second important factor considered in this report is the chemistry of aromatic hydrocarbons with atmospheric reactants. The report includes an investigation of the products of reactions of OH with aromatic hydrocarbons using a low conversion flow system in which OH radicals are produced chemically at low concentrations. Although data on the rate constants of OH reactions with aromatics existed previously, these are the first data on the initial products of these reactions. Since benzaldehyde is a major product of the toluene reaction, we have also investigated the reaction of benzaldehyde with OH.

## 2. CONCLUSIONS AND RECOMMENDATIONS

The results of this work show that PAN is not chemically stable in the atmosphere but is in equilibrium with acetylperoxy radicals and  $\text{NO}_2$  according to the reaction



The dissociation occurs with a lifetime of 30 minutes at  $25^\circ\text{C}$ . At high  $[\text{NO}_2]/[\text{NO}]$  ratios PAN is regenerated following each dissociation of a PAN molecule; however even at  $[\text{NO}_2]/[\text{NO}] = 3$  a PAN molecule is regenerated only one out of two dissociations. This is due to the rapid reaction with NO



which has a rate constant three times faster than the reaction with  $\text{NO}_2$ . When PAN does react with NO it will generate radicals which initiate additional hydrocarbon consumption and NO oxidation. Thus PAN plays an important role in the overall chemistry and especially has a large effect on ozone formation.

Our results on the facile reactions of OH radical with aromatic hydrocarbons show that both oxidation of the ring methyl group and hydroxylation of the ring occur. Thus both substituted benzaldehydes and phenols are the major initial products from the aromatic hydrocarbons. The reaction of benzaldehyde itself with OH is at the aldehydic hydrogen, leading to peroxybenzoyl nitrate and phenol.

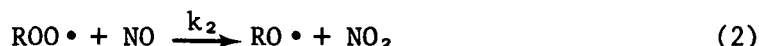
We make two general recommendations with regard to our study. First, the fact that PAN can play an important role in controlling the formation of smog raises the question as to whether other peroxy nitrates can also be important. Therefore a study of the chemistry of other

peroxynitrate compounds should be carried out in order that chemical models that describe photochemical smog formation may be accurate in this regard. Second, the identification of the initial products of the reactions of aromatic compounds with OH under atmospheric conditions is only the first step in understanding the effect of these compounds in the overall smog formation chemistry. Thus the work must be extended to determine the fate of various products that are formed at each stage.

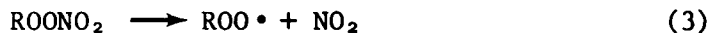
### 3. GAS PHASE FREE RADICAL REACTIONS OF PEROXYACETYL NITRATE

#### INTRODUCTION

The two principal reactions of peroxy radicals in the troposphere are reaction with  $\text{NO}_2$  (reaction 1) and with  $\text{NO}$  (reaction 2).



Reaction 2 is recognized as the primary means by which  $\text{NO}$  is oxidized to  $\text{NO}_2$  and is thereby crucial in establishing elevated levels of ozone in the environment.<sup>1,2</sup> Reaction 1, which is less well recognized, is significant in two respects. First, the products of the reaction, peroxy nitrates ( $\text{ROONO}_2$ ), are themselves noxious pollutants. The best example is peroxyacetyl nitrate ( $\text{CH}_3\text{C}(\text{O})\text{OONO}_2$ ), PAN,<sup>3</sup> which is a frequently observed constituent of photochemical smog,<sup>1,4-12</sup> and a known lachrymator<sup>13</sup> and phytotoxicant.<sup>6,14,15</sup> Second, reaction 1 scavenges peroxy radicals, trapping them as peroxy nitrates and preventing the radicals from reacting with  $\text{NO}$ . However, the peroxy nitrates act as a radical sink only to the extent that they do not undergo homolytic decomposition (reactions 3 and 4):



To determine whether the generalized reaction 3 could play a significant role in the chemistry of polluted urban atmospheres, we have begun an investigation of the gas phase free radical reactions of

peroxy nitrates.<sup>16</sup> This section presents in detail the results of our studies concerning the kinetics and mechanisms of the homolysis of PAN. Also described is the use of PAN as a source of radicals to determine  $k_1$  and  $k_2$ , the rate constants for the reactions of acetylperoxy radicals with  $\text{NO}_2$  and  $\text{NO}$ , respectively.

## EXPERIMENTAL SECTION

### Materials

Peroxyacetic acid was prepared from acetic anhydride,  $\text{H}_2\text{SO}_4$ , and 90%  $\text{H}_2\text{O}_2$ . As described by Swern,<sup>17</sup> the reactants were combined by stirring at  $0^\circ\text{C}$  and then allowed to warm to room temperature overnight. The resulting solution contained 61% peroxyacetic acid and was used without further purification.

Peroxyacetyl nitrate (PAN) was prepared as suggested by Louw et al.<sup>18</sup> and Stephens<sup>3</sup> by the direct nitration of peroxyacetic acid. Thus, 61% peroxyacetic acid, 0.5 g ( $4.1 \times 10^{-3}$  mol), in 30 ml reagent grade pentane was stirred at 0 to  $-5^\circ\text{C}$  under argon. To this mixture, 30%  $\text{SO}_3$ , 2.3 g ( $8.8 \times 10^{-3}$  mol) was added dropwise, followed by 90%  $\text{HNO}_3$ , 0.28 g ( $2 \times 10^{-3}$  mol). After 15 minutes the reaction mixture was washed three times with water, then dried with  $\text{MgSO}_4$ . The ir spectrum of this solution showed the 1835, 1735  $\text{cm}^{-1}$  peaks characteristics of PAN. On the basis of the absorbance of the 1735  $\text{cm}^{-1}$  peak and the extinction coefficient at this frequency,<sup>3</sup> the yield of the reaction was estimated to be 39%.

Gas phase samples of pure PAN were obtained by preparative scale gas liquid partition chromatography (glpc) using the method of Stephens et al.<sup>19</sup> Analysis of PAN purified in this manner showed it to be contaminated with approximately 0.4% pentane. The last traces of pentane could be removed by chromatographing the sample a second time. In kinetic runs, control experiments assured us that the traces of pentane remaining in once-chromatographed PAN had no detectable effect on observed reaction rates.



$\text{NO}_2$  (Matheson) and  $^{15}\text{NO}_2$  (Stohler Isotope Chemicals) were purified to remove NO by combining them with  $\text{O}_2$  and allowing the mixtures to stand 15 minutes before degassing at  $-196^\circ\text{C}$ .

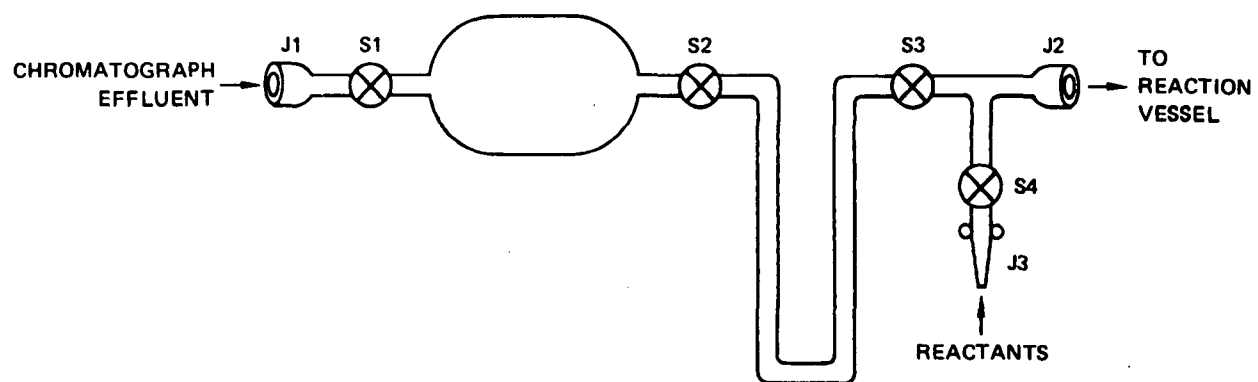
NO (Matheson) was passed through Linde 13X mole sieves, degassed at  $-196^\circ\text{C}$ , and distilled from a liquid oxygen cooled bulb. Acetaldehyde and propanal (Aldrich) were purified by fractional distillation under argon and were degassed before use.

### Apparatus

Three different gas phase ir cells were used. Each was constructed from a 9.0 cm x 1.5 cm i.d., jacketed Pyrex tube, the ends of which were formed from O-ring joints. O-rings and metal brackets were used to secure NaCl plates to the ends of each vessel. Vacuum stopcocks (lubricated with a minimum amount of halocarbon grease) and ground-glass or O-ring joints on each vessel permitted evacuation of the cell and admission of reactants.

Cell II differed from the other two in that its interior surfaces were coated with Teflon. Cells I and III did not differ significantly. As noted in the Results and Discussion Section, cells I and II were used to follow some of the decompositions of PAN in the absence of added reactants. With these exceptions, cell III was used for all the gas phase experiments reported here. Samples of purified PAN were collected in the U-tube depicted in the U-tube depicted in Figure 1. By connecting the O-ring joint, J1, to the glpc effluent, it was possible to collect PAN at  $-196^\circ\text{C}$  between stopcocks S2 and S3 and to collect He in the bulb (volume = 28.4 ml) between S1 and S2. When warmed to ambient temperature, PAN could be admitted into an evacuated vessel by way of J2. Reactants in addition to PAN could be added to the system by S4 and J3. Opening S2 allowed He to enter the vessel as well, resulting in a total pressure of approximately 500 torr.

Helium was used as diluent gas in most of the reactions. The exceptions were a few PAN decompositions in the absence of added reactants to which 1 atm of air was used as diluent (see Table 1).



SA-4466-6

FIGURE 1 U-TUBE FOR COLLECTION OF PAN

Table 1. OBSERVED RATE CONSTANTS ( $k_{\text{obs}}$ ) FOR PAN DECOMPOSITIONS IN THE ABSENCE OF ADDED REACTANTS AT VARIOUS TEMPERATURES

Temperature (°C)	$[\text{PAN}]_0$ $\times 10^4 \text{ M}$	$\overset{\text{a}}{k_{\text{obs}}}$ $\times 10^4 \text{ s}^{-1}$	Cell <sup>b</sup>	Diluent Gas
25	0.809	0.015	III	He
	1.23	0.018	III	He
	1.29	0.011	III	He
	1.41	<u>0.010</u>	III	He
average = 0.014 $\pm$ 0.0032				
48.2	3.35	0.28	III	He
	2.64	0.30	III	He
	2.83	0.18	II	He
	1.18	0.18	II	He
	0.603	<u>0.16</u>	II	He
average = 0.22 $\pm$ 0.06				
57.6	0.711	0.51	I	Air
62.5	0.442	0.77	II	He
67.9	0.480	1.9	I	Air
	0.390	1.7	II	He
	0.635	1.8	I	Air
	0.558	<u>1.7</u>	I	Air
average = 1.8 $\pm$ 0.1				
72.5	0.780	2.9	II	He
	0.407	5.5	I	Air
	0.49	<u>6.8</u>	I	Air
average = 5.1 $\pm$ 1.6				
77.2	0.660	5.9	I	Air
	0.472	5.8	I	Air
82.2	0.405	12	I	Air
	0.405	12	I	Air
92.5	0.405	29	I	Air

<sup>a</sup> $k_{\text{obs}} = (\ln 2)/t_{1/2}$ , where  $t_{1/2}$  is observed half-life for decomposition of pure PAN (see text).

<sup>b</sup>See Experimental Section for description of Cells I through III.

Temperature control was maintained to within  $\pm 0.1^\circ\text{C}$  with a Haake constant temperature circulating bath. Reaction temperatures were measured with a calibrated thermocouple inserted into the jacket surrounding a reaction vessel.

A Perkin-Elmer Model 467 spectrophotometer was used for all ir analyses. The spectrophotometer was coupled to an external recorder for kinetic measurements.

### Procedure

All concentrations of gaseous reactants, except for NO, were determined by ir analysis. Extinction coefficients ( $\epsilon$ ) for PAN given by Stephens<sup>3</sup> are:  $\epsilon_{1835} = 22.4 \times 10^3 \text{ M}^{-1} \text{ m}^{-1}$ ;  $\epsilon_{1735} = 53.0 \times 10^3 \text{ M}^{-1} \text{ m}^{-1}$ . Values of  $\epsilon$  for NO<sub>2</sub> were measured for reaction vessels with and without added diluent. First, NO<sub>2</sub> was added to an evacuated ir cell and the pressure was measured. The concentration of NO<sub>2</sub> was calculated from the pressure and the value of the equilibrium constant for the NO<sub>2</sub>/N<sub>2</sub>O<sub>4</sub> equilibrium at 25°C ( $K_p = 106 \text{ torr}$ ).<sup>20</sup> Next, the absorbance at 1618 cm<sup>-1</sup> was measured with the cell thermostated at 25°C, giving  $\epsilon_{1618} = 6.1 \times 10^3 \text{ M}^{-1} \text{ m}^{-1}$ . Finally, 500 torr of He diluent was added to the cell and the absorbance at 1618 cm<sup>-1</sup> was recalculated. The value of  $\epsilon$  obtained under these conditions was  $\epsilon_{1618} = 21.7 \times 10^3 \text{ M}^{-1} \text{ m}^{-1}$ . The 1590 cm<sup>-1</sup> extinction coefficients for <sup>15</sup>NO<sub>2</sub> were assumed to be equal to the values measured for NO<sub>2</sub> at 1618 cm<sup>-1</sup>. To determine the extinction coefficients for CH<sub>3</sub>CHO, we measured amounts of CH<sub>3</sub>CHO in a gas buret and transferred them into a reaction vessel with a Toepler pump. The vessel was pressurized to 500 torr with He, and the absorbances were measured at 2750 and 1770 cm<sup>-1</sup>. Values of  $\epsilon$  were found to be:  $\epsilon_{2750} = 2.84 \times 10^3 \text{ M}^{-1} \text{ m}^{-1}$ ;  $\epsilon_{1770} = 9.53 \times 10^3 \text{ M}^{-1} \text{ m}^{-1}$ . C<sub>2</sub>H<sub>5</sub>CHO was assumed to exhibit values of  $\epsilon$  identical to those for CH<sub>3</sub>CHO. Amounts of NO were determined with a gas buret and transferred to an evacuated reaction vessel with a Toepler pump.

For the reaction of <sup>15</sup>NO<sub>2</sub> with PAN, kinetics were determined in the following manner. <sup>15</sup>NO<sub>2</sub> was added to the evacuated cell and its concentration

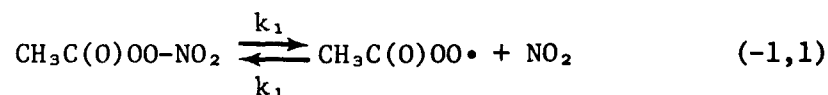
was measured. The cell was thermostated and placed in the spectrophotometer, PAN and He were added, and the  $1900\text{ cm}^{-1}$  to  $1500\text{ cm}^{-1}$  region of the spectrum was immediately scanned. This region was then repeatedly scanned at approximately 10-minute intervals. Spectrophotometer output was registered on a continuously moving remote recorder and the change in absorbance of any reactant could be measured as a function of time.

Concentrations of PAN used in the gas phase experiments typically ranged from  $0.5$  to  $2.5 \times 10^{-4}$  M. For a 25 ml reaction vessel, it was therefore never necessary to handle more than approximately  $6 \times 10^{-6}$  moles of the potentially dangerous<sup>21</sup> PAN vapor. Moreover, these concentrations were well below the vapor pressure of PAN, reported<sup>3</sup> to be 15 to 20 torr ( $8$  to  $10^{-4}$  M at  $25^\circ\text{C}$ ).

Solution phase decompositions were performed using samples of PAN prepared as described in the Materials section but substituting  $\text{CCl}_4$  for pentane as solvent. Samples were purified by column chromatography (silica gel at  $0^\circ\text{C}$ ) and weighed into nuclear magnetic resonance (nmr) tubes.  $\text{CHCl}_3$  and  $t\text{-C}_4\text{H}_9\text{OH}$  (internal standard) were also added and weighed as needed. The tubes were then degassed, sealed, and placed in a thermostated bath. Kinetics were measured by withdrawing the samples from the bath at time intervals and recording the nmr spectra.

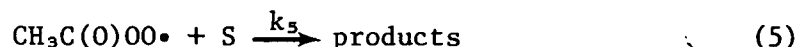
## RESULTS AND DISCUSSION

The thermal decomposition of peroxy nitrates can proceed by two possible pathways. These are O-O homolysis (reaction 4) and O-N homolysis (reaction 3), the reverse of the reaction by which peroxy nitrates are formed. In the case of PAN itself, homolytic bond scission (reaction -1) produces acetylperoxy radicals and  $\text{NO}_2$ .

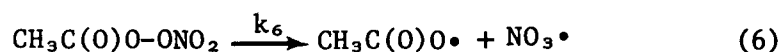


Because acetylperoxy radicals are not prone to unimolecular decomposition, they are relatively long lived, and reaction 1, the reverse of the homolysis,

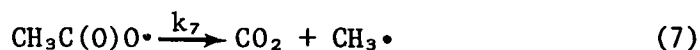
must also be considered. In effect, this requires that O-N homolysis involve a dynamic equilibrium between PAN, acetylperoxy radicals, and NO<sub>2</sub>. Net decomposition of a molecule of PAN could occur only after destruction of an acetylperoxy radical by a subsequent reaction with a species other than NO<sub>2</sub>.



For the case of O-O homolysis, which is typical of peroxides, the initial products of the bond cleavage are acetoxy radicals and NO<sub>3</sub>.

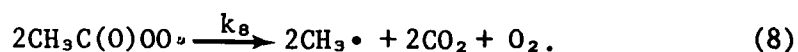


Decarboxylation of acetoxy radicals is unimolecular.



This reaction occurs fast enough<sup>22-24</sup> ( $k_7 = 10^9 \text{ s}^{-1}$ ) to preclude bimolecular reactions. Thus, the reverse of reaction 5 need not be considered, and decomposition of PAN by O-O homolysis could not involve an equilibrium between PAN and radical species.

To probe the precise mechanism of PAN homolysis, we have investigated the rate of thermal decomposition of PAN in the absence and presence of free radical scavengers. In the absence of scavengers, decomposition of PAN by reaction 6 requires that the disappearance of PAN obey strictly first-order kinetics. If O-N homolysis predominates, decomposition of pure PAN will proceed by reactions -1, 1, and 8.



In this case, the steady-state expression for disappearance of PAN contains quadratic terms and the observed rate of decomposition need not be first-order in [PAN].

When PAN decomposes in the presence of a radical scavenger, S, the rate of disappearance of PAN by reaction 6 will be identical to the rate observed in the absence of the scavenger. That is, the presence of a scavenger will affect neither reaction 6 nor reaction 7. On the other hand, if decomposition involves the equilibrium -1,1, scavengers can intercept acetylperoxy radicals (reaction 5), shifting the equilibrium to the right and enhancing the observed rate of PAN decomposition.

#### Decomposition of Pure PAN

The decomposition of pure gaseous PAN was investigated over the temperature range 25 to 92.5°C. Reproducible rates of decomposition could be obtained at any temperature or in any of three reaction cells, provided the vessels had been "seasoned" by repeated PAN decompositions. Decomposition rates were found to deviate significantly from first-order kinetics. Semilogarithmic plots of the fraction of PAN remaining ( $[\text{PAN}]_t/[\text{PAN}]_0$ ) versus time typically exhibited pronounced upward curvature. Curvature was evident in all decompositions performed, and the degree of curvature could not be correlated with temperature or initial reactant concentration. As discussed above, this type of behavior is consistent with O-N but not with O-O cleavage being the primary mechanism for PAN homolysis.

Except for the 25°C experiments, decompositions were followed to at least 50% of completion and observed half-times ( $t_{1/2}$ ) for decomposition were obtained directly. At 25°C, semilogarithmic plots were extrapolated to 50% decomposition to find values for  $t_{1/2}$ . From the half-times, values of  $k_{\text{obs}}$ , observed rate constant for decomposition of pure PAN, were calculated from the expression:  $k_{\text{obs}} = (\ln 2)/t_{1/2}$ . These  $k_{\text{obs}}$  values (see Table 1) have the dimensions of a first-order rate constant but do not represent a true first-order process because of the curvature in the logarithmic plot.

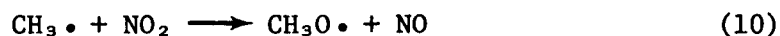
From Table 1 it is evident that reproducible rates of PAN decomposition could be obtained using seasoned reaction vessels made either of Pyrex (cells I and III) or Teflon-coated Pyrex (cell II). This suggests

that the nature of the seasoned vessel surface is not important in determining the rate of PAN decay.

Moreover, a plot (not shown) of  $\ln(k_{\text{obs}})$  versus reciprocal absolute temperature is linear (slope =  $12.36 \pm 0.34 \times 10^4$ , intercept =  $27.79 \pm 1.0 \text{ s}^{-1}$ ,  $r^2 = 0.984$ ) over the entire 25 to 92.5°C temperature range.

Products of PAN decompositions at various temperatures were studied by ir and glpc. Analysis by ir showed peaks due to  $\text{CO}_2$  ( $2320 \text{ cm}^{-1}$ ),  $\text{CH}_3\text{ONO}_2$  (1680, 1660, 1290, 1020,  $850 \text{ cm}^{-1}$ ),<sup>25</sup> and inorganic nitrate ( $1360 \text{ cm}^{-1}$ ).<sup>26</sup> Analysis by glpc confirmed that  $\text{CH}_3\text{ONO}_2$  and  $\text{CH}_3\text{NO}_2$  were present in approximately equal amounts. This type of product distribution was seen for all reactions in which He was the diluent gas. With air as diluent, no  $\text{CH}_3\text{NO}_2$  was observed, and  $\text{CO}_2$ ,  $\text{CH}_3\text{ONO}_2$  and  $\text{NO}_3^-$  were the major products.

$\text{CH}_3\text{ONO}_2$ ,  $\text{CH}_3\text{NO}_2$ , and  $\text{CO}_2$  are indicative of formation of  $\text{CH}_3$  by either O-O cleavage, followed by reaction 7, or O-N cleavage, followed by reaction 8. Reactions 9 through 11 explain the formation of  $\text{CH}_3\text{NO}_2$  and  $\text{CH}_3\text{ONO}_2$ .<sup>27-29</sup>



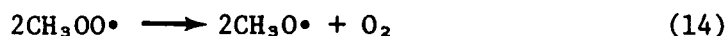
If  $\text{NO}_3$  is present from O-O cleavage, an additional possible source of  $\text{CH}_3\text{ONO}_2$  is



In the presence of large amounts of  $\text{O}_2$ , reactions 9 and 10 are replaced by

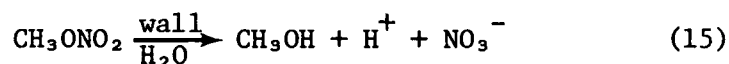




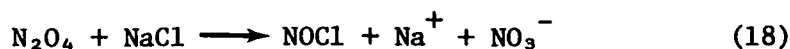
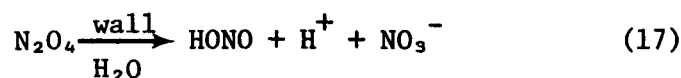


With He as diluent, small amounts of  $\text{O}_2$  are formed and reactions 9 and 13 could compete, but in the presence of air, only reaction 13 would occur, eliminating  $\text{CH}_3\text{NO}_2$  as a reaction product.

Inorganic nitrate was produced on the reaction cell windows in all PAN decompositions. Surface decomposition of PAN is a possible, but not very probable, source of  $\text{NO}_3^-$ , since surface effects on the rate of PAN decay could not be demonstrated. More likely,  $\text{NO}_3^-$  results from surface reactions of  $\text{CH}_3\text{ONO}_2$  and  $\text{NO}_2$ . For  $\text{CH}_3\text{ONO}_2$  produced by PAN decomposition at  $25^\circ\text{C}$  in a control experiment, the reaction of  $\text{CH}_3\text{ONO}_2$  with surface adsorbed moisture



was shown to occur. Analysis by glpc clearly showed that the  $\text{CH}_3\text{ONO}_2$  was unstable under the reaction conditions, decomposing slowly to give  $\text{CH}_3\text{OH}$ . Inorganic nitrate was also produced under these conditions, but we did not quantitatively measure the amount of  $\text{NO}_3^-$  formed relative to the amount of  $\text{CH}_3\text{ONO}_2$  lost. The possibility of nitrate production from  $\text{NO}_2$  was directly demonstrated by simply admitting  $\text{NO}_2$  to a reaction cell, allowing it to stand at  $25^\circ\text{C}$  for several hours, and observing an increase in the absorbance of the  $1360\text{ cm}^{-1}$  peak. Here, nitrate production could be explained by the following reactions:



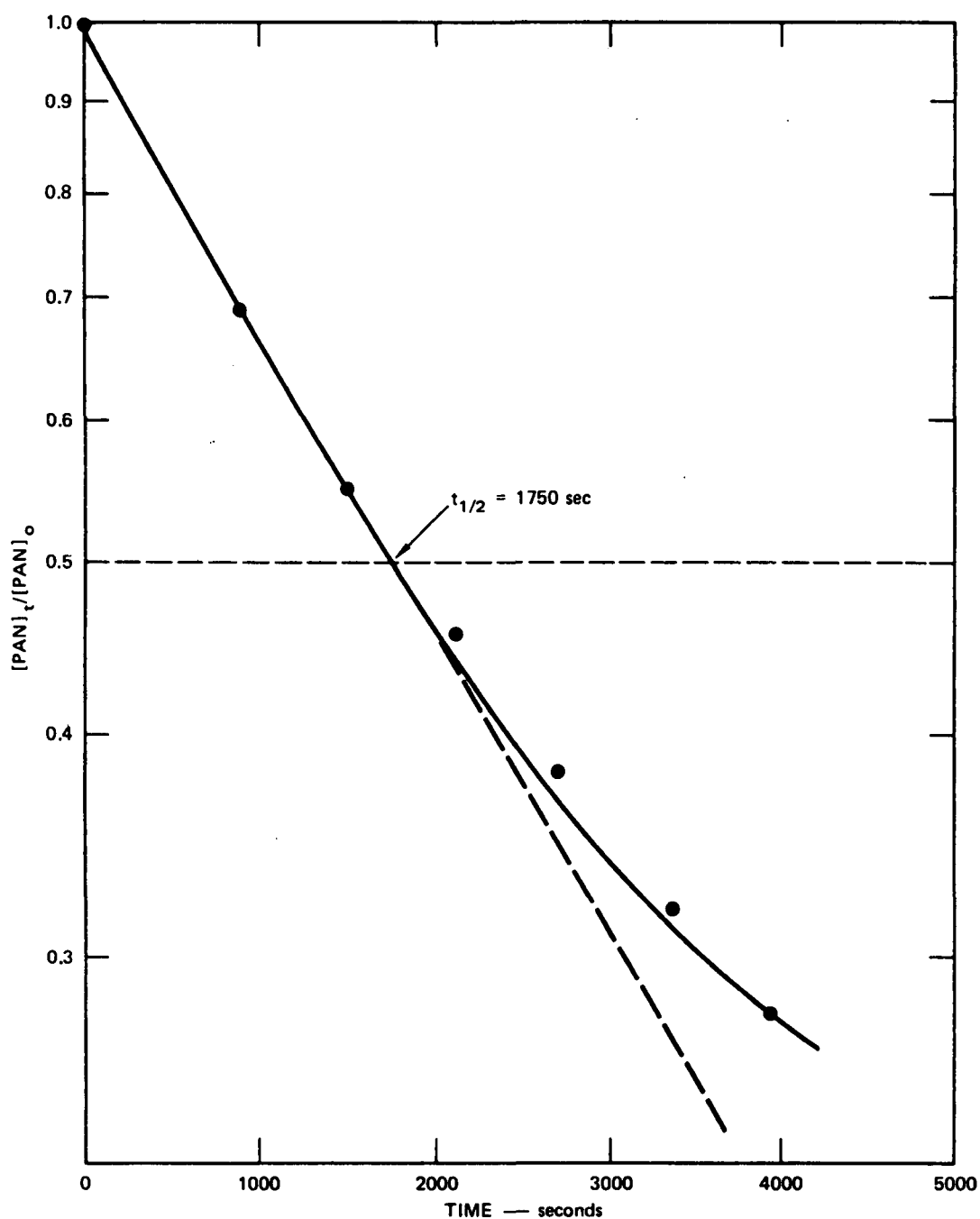
### Decomposition of PAN in the Presence of NO

The effect of radical traps on the rate of PAN decomposition was first investigated using NO as the scavenger. Decomposition rates were determined at temperatures ranging from 25 to 39°C and for [NO]/[PAN] ratios varying as much as ten-fold. Semilogarithmic plots of  $[\text{PAN}]_t/[\text{PAN}]_0$  versus time (see Figure 2) were linear in the initial stages of the reaction but exhibited upward curvature as the reaction progressed. The onset of curvature depended on the [NO]/[PAN] ratio, curvature appearing sooner at low [NO]/[PAN]. Half-times for PAN decompositions were obtained from the initial linear regions of the semilogarithmic plots (extrapolating when necessary) and were used to calculate values for  $k_{\text{obs}}^{\text{NO}}$ , the observed first-order rate constant for decomposition of PAN in the presence of NO. Experimental conditions and  $k_{\text{obs}}^{\text{NO}}$  values are summarized in Table 2. Infrared spectra of the products of the decomposition of PAN in the presence of NO revealed the presence of NO<sub>2</sub> in addition to CO<sub>2</sub> and CH<sub>3</sub>ONO<sub>2</sub>. CH<sub>3</sub>ONO, CH<sub>3</sub>NO, and CH<sub>3</sub>NO<sub>2</sub> may also have been present, but interference from NO<sub>2</sub> and CH<sub>3</sub>ONO<sub>2</sub> absorbances precluded positive identification of these species.

Comparison of the data in Tables 1 and 2 shows that NO has a pronounced effect on the rate of PAN decomposition. At 25°C the rate constants for PAN decomposition are  $1.4 (\pm 0.3) \times 10^{-6} \text{ s}^{-1}$  in the absence of NO and  $3.7 (\pm 0.4) \times 10^{-4} \text{ s}^{-1}$  in the presence of NO. At the same time, the values of  $k_{\text{obs}}^{\text{NO}}$  are independent of the initial [NO]/[PAN] ratio.

Since NO can have no effect on the rate of O-O bond scission, reaction 6 cannot explain the accelerating effect of NO. On the other hand, the data are entirely consistent with reversible O-N cleavage as the primary mechanism for PAN homolysis. To account for the effect of NO on the kinetics of the PAN decomposition, we apply a steady-state analysis to reactions -1, 1 and 5. Thus, noting that reactions 5 and 2 are identical if S = NO and ROO• = CH<sub>3</sub>C(O)OO•, we obtain:

$$-d[\text{PAN}]/dt = [\text{PAN}]k_{-1}\{k_2[\text{NO}]/(k_1[\text{NO}_2] + k_2[\text{NO}])\} \quad (19)$$



SA-4466-1

FIGURE 2 FRACTION OF PAN REMAINING ( $[PAN]_t/[PAN]_o$ ) VERSUS TIME FOR DECOMPOSITION OF  $1.72 \times 10^{-4}$  M PAN IN THE PRESENCE OF  $4.1 \times 10^{-4}$  M NO AT  $25^\circ\text{C}$

Table 2. OBSERVED FIRST-ORDER RATE CONSTANTS,  $k_{\text{obs}}^{\text{NO}}$  FOR DECOMPOSITION OF PAN IN THE PRESENCE OF NO AT VARIOUS TEMPERATURES

Temperature (°C)	$[\text{PAN}]$ $\text{M} \times 10^4$	$[\text{NO}]/[\text{PAN}]$	$k_{\text{obs}}^{\text{NO}}$ $\times 10^4 \text{ s}^{-1}$
25	1.72	2.4	3.96 <sup>b</sup>
	1.89	9.2	3.98
	1.37	1.9	3.21
	3.60	5.6	4.11
	0.99	0.16	<u>3.25</u>
			average = 3.70 ± 0.39
29.9	1.97	2.5	8.82
	1.98	4.8	7.67
	1.36	7.2	<u>7.91</u>
			average = 8.13 ± 0.50
34.3	1.10	1.5	12.3
	1.46	16.	14.2
	1.21	3.6	<u>15.4</u>
			average = 14.0 ± 1.3
39.0	1.58	5.6	28.8
	1.44	0.68	28.5
	1.29	8.5	<u>29.6</u>
			average = 29.0 ± 0.5

<sup>a</sup>  $k_{\text{obs}}^{\text{NO}}$  determined from linear region of  $\log [\text{PAN}]_t/[\text{PAN}]_0$  versus time plot (see text).

<sup>b</sup> Data of Figure 2.

When  $k_2[\text{NO}] \gg k_1[\text{NO}_2]$ , equation 19 reduces to:

$$-d[\text{PAN}]/dt = [\text{PAN}]k_{-1} = [\text{PAN}]k_{\text{obs}}^{\text{NO}} \quad (20)$$

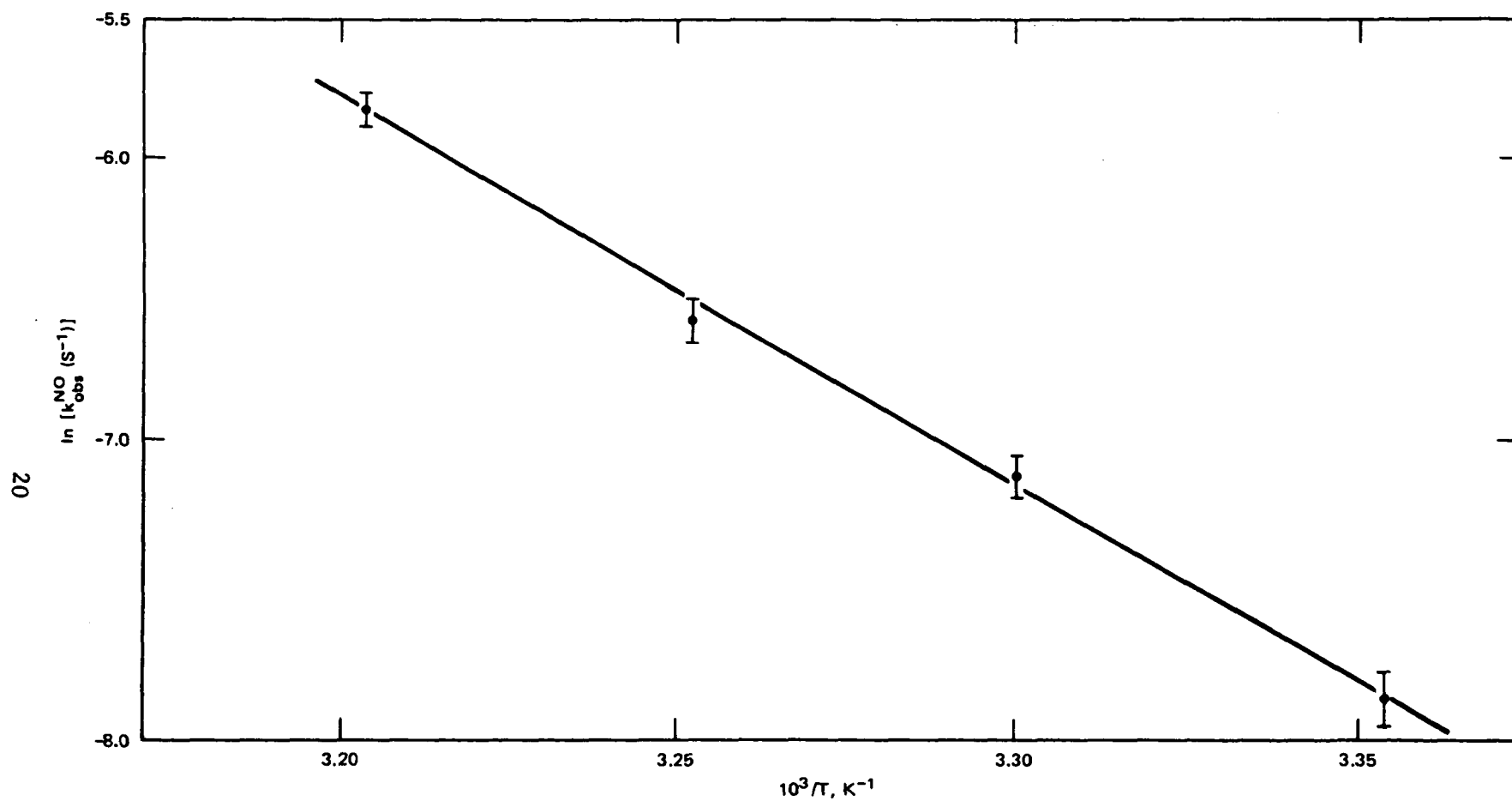
Here, the rate of PAN decay is first-order in PAN and zero-order in NO, as is observed in the initial stages of the reactions. However, as the decomposition proceeds, NO is oxidized to NO<sub>2</sub> by reaction 2, and eventually the point is reached at which  $k_1[\text{NO}_2]$  is no longer negligible compared with  $k_2[\text{NO}]$ . In this case, equation 20 fails and  $k_{\text{obs}}^{\text{NO}}$  is less than  $k_{-1}$  by the factor  $k_2[\text{NO}]/(k_1[\text{NO}_2] + k_2[\text{NO}])$ .

Figure 3 is an Arrhenius plot of the average  $k_{\text{obs}}^{\text{NO}}$  values taken from Table 2. Because all the data in Table 2 correspond to the case where  $k_2[\text{NO}] \gg k_1[\text{NO}_2]$ , equation 20 holds and  $k_{\text{obs}}^{\text{NO}}$  equals  $k_{-1}$  at each temperature. For this reason, the slope and intercept of Figure 3 can be used to derive the activation parameters for O-N homolysis; thus,  $k_{\text{obs}}^{\text{NO}}$  (s<sup>-1</sup>) equals  $(10^{16.29 \pm 0.60}) \exp(26910 \pm 900)/\theta$ , where  $\theta$  equals 2.303 RT in calories per mole.

#### Decomposition of PAN in the Presence of Hydrogen Atom Donors

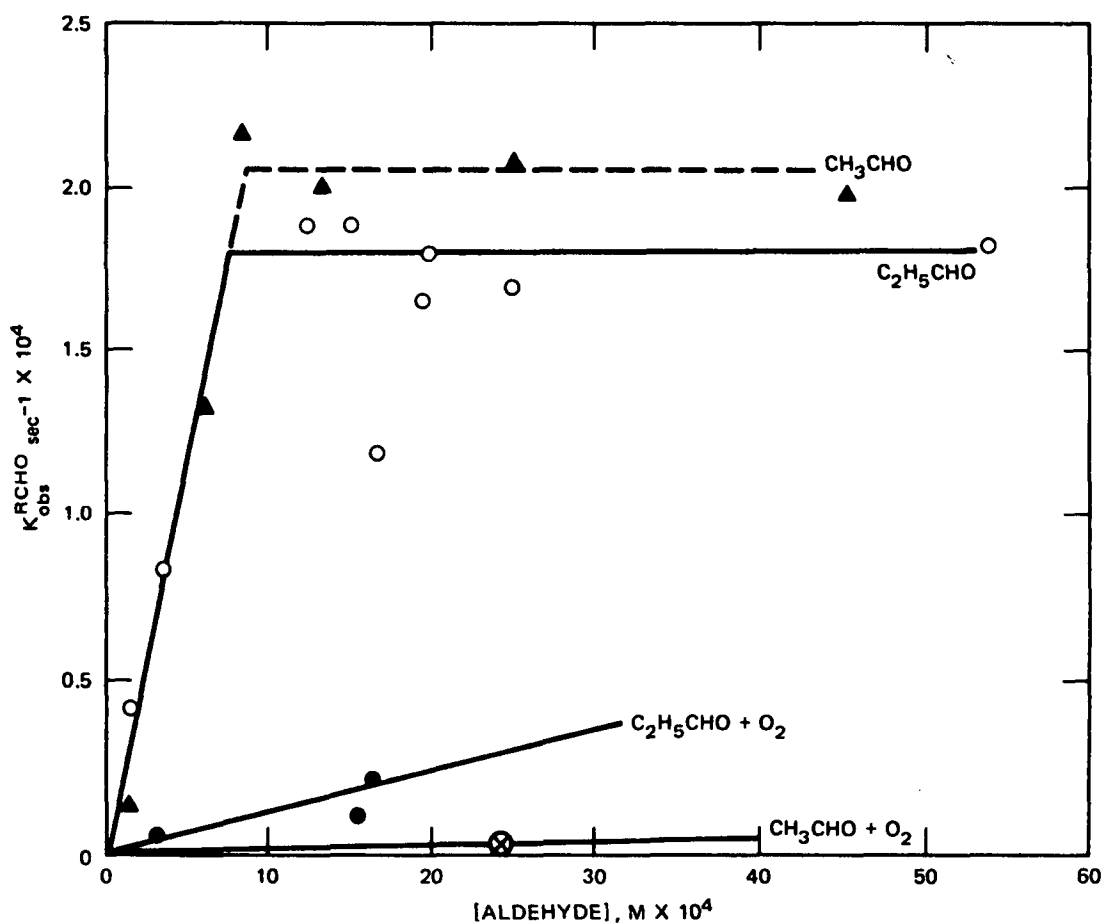
To establish the general nature of reaction 5, we followed PAN decompositions at 25°C in the presence of added hydrogen atom donors. The intent was to demonstrate an accelerated rate of PAN decomposition and also to provide direct evidence for the intermediacy of acetylperoxy radicals by trapping them as peroxyacetic acid.

The two hydrogen atom donors most extensively investigated were CH<sub>3</sub>CHO and C<sub>2</sub>H<sub>5</sub>CHO. PAN decompositions were followed at 25°C in the presence of excess aldehyde ( $[\text{RCHO}]/[\text{PAN}]$  ranging from 1.05 to 27) with either He or oxygen as diluent. Semilogarithmic plots of  $[\text{PAN}]_t/[\text{PAN}]_0$  versus time were linear for at least 70% reaction, and half-times for PAN decay were used to calculate  $k_{\text{obs}}^{\text{RCHO}}$ , the observed first-order rate constant for the decomposition of PAN in the presence of aldehyde. Values of  $k_{\text{obs}}^{\text{RCHO}}$  are plotted versus concentration of aldehyde in Figure 4.



SA-4466-5

FIGURE 3  $\ln(k_{\text{obs}}^{\text{NO}})$  VERSUS  $1/T$  (K<sup>-1</sup>) FOR DECOMPOSITION OF PAN IN THE PRESENCE OF NO  
Slope =  $(1.35 \pm 0.05) \times 10^4$ . Intercept =  $37.44 \pm 1.38$ .



SA-4466-7

FIGURE 4 OBSERVED FIRST-ORDER RATE CONSTANTS,  $k_{obs}^{RCHO}$  FOR DECOMPOSITION OF PAN AT 25°C IN THE PRESENCE OF: CH<sub>3</sub>CHO WITH (⊗-⊗) AND WITHOUT (▲-▲) ADDED O<sub>2</sub>; AND C<sub>2</sub>H<sub>5</sub>CHO WITH (●-●) AND WITHOUT (○-○) ADDED O<sub>2</sub>

Products of the decompositions in the presence of aldehydes were shown by ir to be CO<sub>2</sub>, alkyl nitrates, and nitroalkane, which was observed only in the absence of added oxygen. Peroxyacetic acid was not observed to be a product of the decompositions, although small amounts of the peracid might have gone undetected because of interference from aldehyde absorption bands.

A mechanism that is consistent with these results involves the equilibrium -1,1 and reaction 5 where S equals RCHO. For this mechanism, the rate of disappearance of PAN is governed by equation 21.

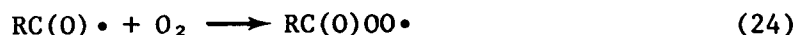
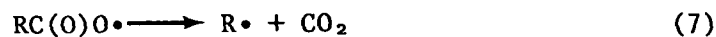
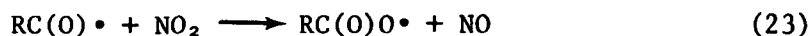
$$-d[\text{PAN}]/dt = [\text{PAN}]k_{-1}\{k_5^{\text{RCHO}}[\text{RCHO}]/(k_5^{\text{RCHO}}[\text{RCHO}] + k_1[\text{NO}_2])\} \quad (21)$$

Equation 21 predicts that when  $k_5^{\text{RCHO}}[\text{RCHO}] \gg k_1[\text{NO}_2]$ , PAN decomposition will follow equation 22

$$-d[\text{PAN}]/dt = [\text{PAN}]k_{-1} = [\text{PAN}]k_{\text{obs}}^{\text{RCHO}} \quad (22)$$

Figure 4 shows that the rate of PAN decomposition becomes zero-order in [aldehyde], in apparent agreement with equation 22. However, the maximum values obtained for  $k_{\text{obs}}^{\text{RCHO}}$  (approximately  $2 \times 10^{-4} \text{ s}^{-1}$ ) are significantly lower than the value of  $k_{-1} = 3.7 \pm 0.39 \times 10^{-4} \text{ s}^{-1}$  determined for PAN decomposition in the presence of NO. Also, adding O<sub>2</sub> to the PAN/RCHO system is seen to lower the value of  $k_{\text{obs}}^{\text{RCHO}}$  relative to the value obtained with He diluent.

These observations can be rationalized by expanding the mechanism for the PAN/RCHO system to include reactions 23, 7, and 24.





If reaction 23 does occur, NO is produced and reaction 2 must also be considered. In this case the rate of disappearance of PAN is given by equation 25.

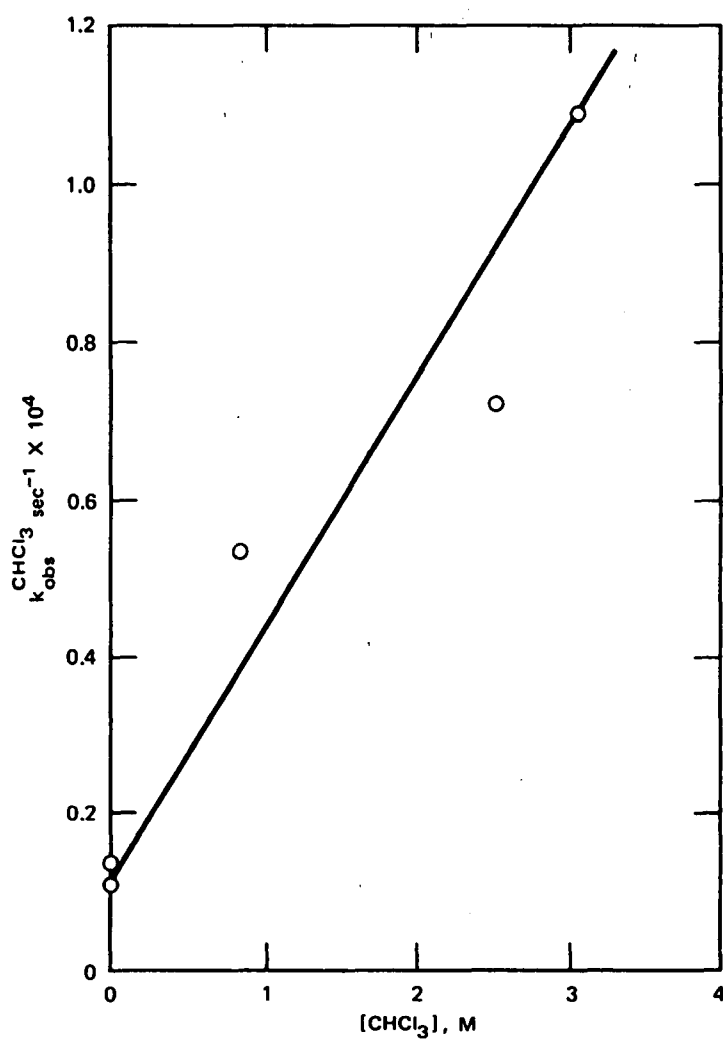
$$-d[\text{PAN}]/dt = [\text{PAN}]k_{-1}\{(k_5^{\text{RCHO}}[\text{RCHO}] + k_2[\text{NO}]/(k_5^{\text{RCHO}}[\text{RCHO}] + k_2[\text{NO}] + k_1[\text{NO}_2]))\} \quad (25)$$

When  $k_2[\text{NO}]$  greatly exceeds  $k_5^{\text{RCHO}}[\text{RCHO}]$  but not  $k_1[\text{NO}_2]$ , equation 25 becomes

$$-d[\text{PAN}]/dt = [\text{PAN}]k_{-1}\{k_2[\text{NO}]/(k_2[\text{NO}] + k_1[\text{NO}_2])\} = [\text{PAN}]k_{\text{obs}}^{\text{RCHO}} \quad (26)$$

In this manner, it is possible to explain the zero-order dependence of  $k_{\text{obs}}^{\text{RCHO}}$  on  $[\text{RCHO}]$  and the discrepancy between  $k_{\text{obs}}^{\text{RCHO}}$  and  $k_{-1}$ . When  $\text{O}_2$  is added to the system, reaction 24<sup>30</sup> occurs to the exclusion of reaction 23 and the rate of PAN decay adheres to equation 21. The value of  $k_5^{\text{RCHO}}$  is so low ( $k_5^{\text{RCHO}} \approx 10^3 \text{ M}^{-1} \text{ s}^{-1}$  for solution phase aldehyde autoxidations at  $0^\circ$ )<sup>31</sup> that concentrations of aldehyde leading to equation 22 could not be achieved under gas phase conditions. For the particular case of the PAN/ $\text{CH}_3\text{CHO}/\text{O}_2$  system, reactions 5 and 24 yield acetylperoxy radicals that can reform PAN by reaction 1. Thus no decrease in  $[\text{PAN}]$  was observed during the time when this reaction was studied.

The effect of hydrogen atom donors on the rate of PAN decomposition was also investigated in solution at  $55^\circ\text{C}$ . Here  $\text{CCl}_4$  served as solvent and  $\text{CHCl}_3$  as the hydrogen atom donor. Nuclear magnetic resonance was used to monitor the rate of disappearance of  $5$  to  $8 \times 10^{-2} \text{ M}$  PAN in the presence of varying  $[\text{CHCl}_3]$ . Semilogarithmic plots of  $[\text{PAN}]_t/[\text{PAN}]_0$  versus time were linear for at least 85% reaction. Observed half-times were used to find first-order rate constants,  $k_{\text{obs}}^{\text{CHCl}_3}$ , for decomposition in the presence of  $\text{CHCl}_3$ . These values are plotted versus  $[\text{CHCl}_3]$  in Figure 5. For increasing  $[\text{CHCl}_3]$ ,  $k_{\text{obs}}^{\text{CHCl}_3}$  is seen to increase, in accordance with equation 21, where  $\text{CHCl}_3$  is substituted for RCHO.



SA-4466-3

FIGURE 5 OBSERVED FIRST-ORDER RATE CONSTANTS,  $k_{\text{obs}}^{\text{CHCl}_3}$ , FOR THE DECOMPOSITION OF PAN AT 55°C IN  $\text{CHCl}_3/\text{CCl}_4$  SOLUTIONS  
 Slope =  $(2.75 \pm 0.45) \times 10^{-5} \text{ M}^{-1} \text{ s}^{-1}$ . Intercept =  $(1.66 \pm 0.84) \times 10^{-5} \text{ s}^{-1}$ .

Products of the decomposition of PAN in  $\text{CCl}_4$  containing no  $\text{CHCl}_3$  were found (by nmr, ir, and ms) to be  $\text{CO}_2$ ,  $\text{CH}_3\text{Cl}$ ,  $\text{CH}_3\text{ONO}_2$ , and  $\text{CH}_3\text{NO}_2$ . For solutions containing  $\text{CHCl}_3$ , the products were  $\text{CO}_2$ ,  $\text{CH}_3\text{Cl}$ ,  $\text{CH}_3\text{NO}_2$ ,  $\text{CH}_4$ ,  $\text{CH}_3\text{OH}$ , and  $\text{CH}_3\text{C}(\text{O})\text{OOH}$ . The presence of the peracid was clearly indicated by an nmr singlet at 128 cps (downfield from TMS) and ir absorption bands at 1785 and 1445  $\text{cm}^{-1}$ .

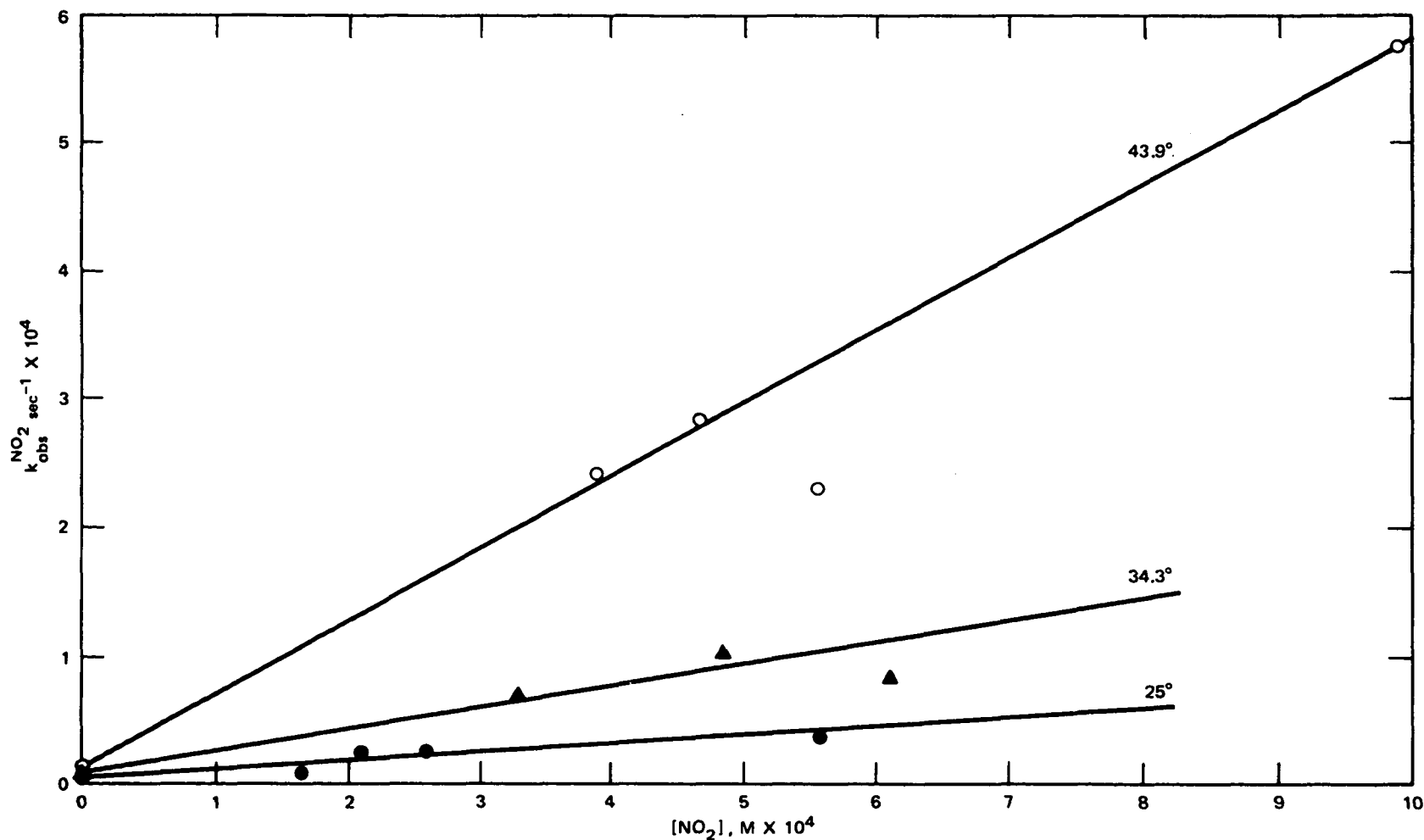
These results demonstrate that PAN generated acetylperoxy radicals and indicate that reactions -1, 1 and 5 are important for the decomposition of PAN under a variety of conditions.

#### Decomposition of PAN in the Presence of $\text{NO}_2$ and $^{15}\text{NO}_2$

To further characterize the mechanism of PAN homolysis, we performed a series of decompositions in the presence of added  $\text{NO}_2$ . It was anticipated that  $\text{NO}_2$  would suppress the rate of PAN decomposition by increasing the importance of reaction 1 relative to reaction -1. Contrary to these expectations,  $\text{NO}_2$  in some cases actually enhanced the rate of PAN decomposition. Semilogarithmic plots of  $[\text{PAN}]_t/[\text{PAN}]_0$  versus time exhibited varying degrees of curvature and, as was done for pure PAN decompositions, observed half-times were used to calculate  $k_{\text{obs}}^{\text{NO}_2}$ , the rate constants for PAN decomposition in the presence of  $\text{NO}_2$ . Values of  $k_{\text{obs}}^{\text{NO}_2}$  obtained at three temperatures and at  $[\text{NO}_2]/[\text{PAN}]$  ratios ranging from 1 to 14 are plotted versus  $[\text{NO}_2]$  in Figure 6.

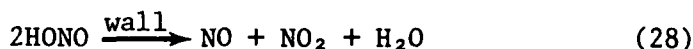
We attribute these results to the presence of NO in the PAN plus  $\text{NO}_2$  system. The effect of NO would be to accelerate the rate of PAN decomposition, as described above. A possible source of NO is surface decomposition of  $\text{NO}_2$  by reactions 16 through 18. These reactions were previously postulated to explain the formation of  $\text{NO}_3^-$  on reaction cell windows. In addition to inorganic nitrate, HONO and NOCl are products of reactions 17 and 18, respectively. These products could be converted to NO by reactions 27<sup>32</sup> and 28.<sup>33</sup>





SA-4466-4

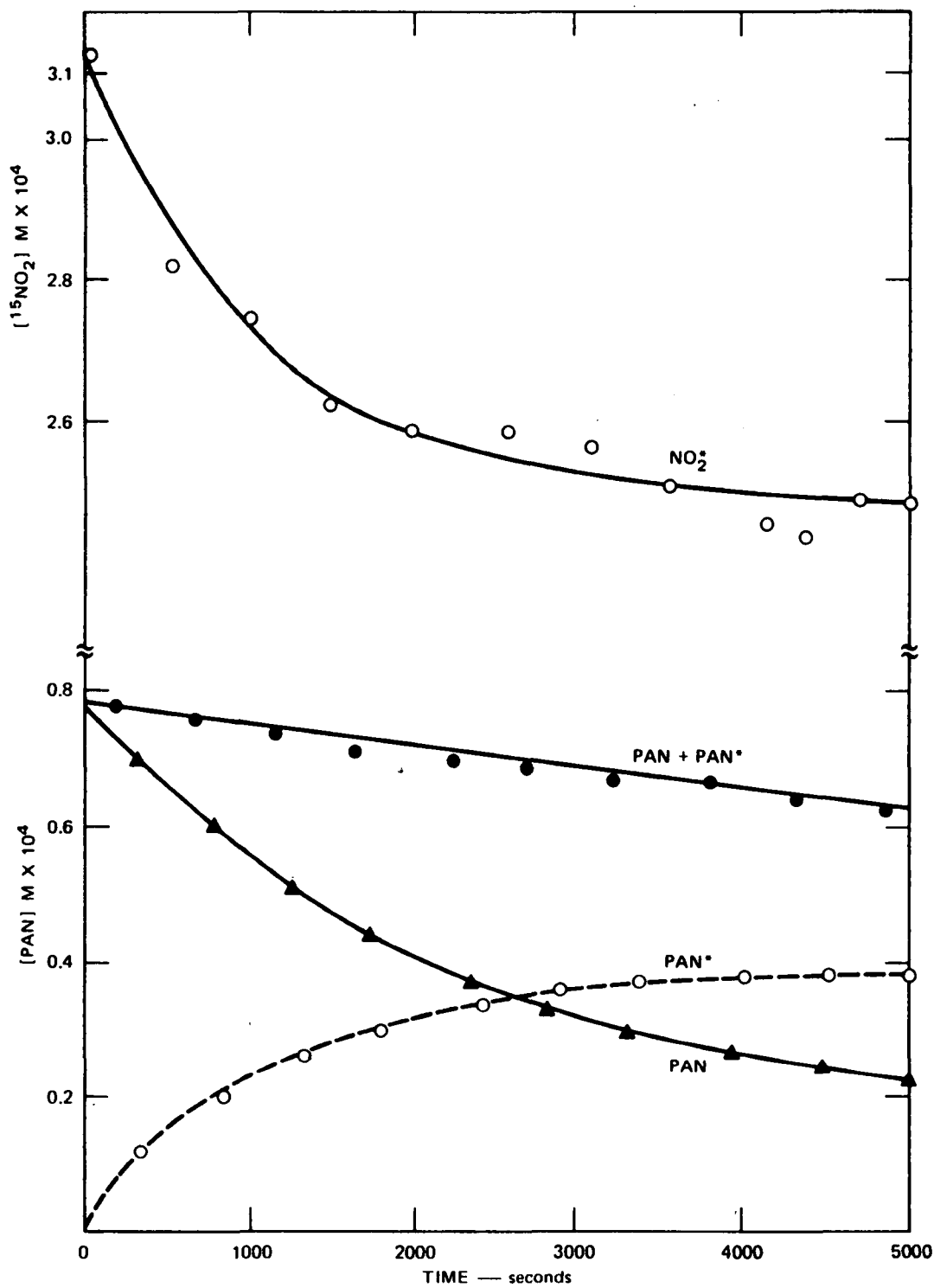
FIGURE 6 OBSERVED RATE CONSTANT,  $k_{\text{obs}}^{\text{NO}_2}$ , VERSUS  $[\text{NO}_2]$  FOR DECOMPOSITION OF PAN IN THE PRESENCE OF ADDED  $\text{NO}_2$  AT: 25°C (●-●), SLOPE =  $(0.064 \pm 0.015) \times 10^{-4} \text{ M}^{-1} \text{ s}^{-1}$ ; INTERCEPT =  $(0.015 \pm 0.05) \times 10^{-4} \text{ s}^{-1}$ ; 34.3°C (▲-▲), SLOPE =  $(0.21 \pm 0.04) \times 10^{-4} \text{ M}^{-1} \text{ s}^{-1}$ ; INTERCEPT =  $(0.045 \pm 0.15) \times 10^{-4} \text{ s}^{-1}$ ; AND 43.9°C (○-○), SLOPE =  $(0.55 \pm 0.07) \times 10^{-4} \text{ M}^{-1} \text{ s}^{-1}$ ; INTERCEPT =  $(0.030 \pm 0.4) \times 10^{-4} \text{ s}^{-1}$ .



An alternative explanation regarding the PAN/NO<sub>2</sub> system is that side reactions such as 17, 18, 27 and 28 are not involved and that the rate enhancement caused by NO<sub>2</sub> is an indication of the failure of reactions -1,1 and 6 to describe accurately the mechanism of PAN homolysis. To eliminate this possibility, we studied the decomposition of PAN at 25°C in the presence of added <sup>15</sup>N-labeled NO<sub>2</sub> (NO<sub>2</sub><sup>\*</sup>). Our intent was to demonstrate that the equilibrium -1, 1 and any surface reactions involving NO would occur simultaneously. The side reactions would be indicated by an increase in the rate of disappearance of total PAN relative to the rate of disappearance of PAN in the absence of NO<sub>2</sub>. The equilibrium -1,1 would be directly demonstrated by trapping acetylperoxy radicals with NO<sub>2</sub><sup>\*</sup> to form <sup>15</sup>N-labeled PAN (PAN<sup>\*</sup>).

The method used to study the PAN/NO<sub>2</sub><sup>\*</sup> system was to repeatedly scan the 1900 to 1500 cm<sup>-1</sup> region of the ir spectrum at timed intervals. This technique is based on the different ir absorption frequencies exhibited by labeled and unlabeled PAN and NO<sub>2</sub> (see Table 3). By measuring the absorbances at 1835, 1734, 1696, and 1590 cm<sup>-1</sup> at different times, it was possible to determine the concentrations of total PAN (PAN + PAN<sup>\*</sup>) and NO<sub>2</sub><sup>\*</sup>, respectively. Concentrations of NO<sub>2</sub> could also be measured using the 1618 cm<sup>-1</sup> absorption frequency, but these values were inaccurate because of interference from the strong NO<sub>2</sub><sup>\*</sup> absorbance centered at 1590 cm<sup>-1</sup>.

Results for a typical experiment are shown in Figure 7. From the figure, it is evident that the concentration of total PAN decreases. By extrapolation of the line for [PAN] + [PAN<sup>\*</sup>], the half-time for decomposition of total PAN is found to be 1.73 x 10<sup>4</sup> s. This equates to a rate constant of 4.0 x 10<sup>-5</sup> s<sup>-1</sup>, in fair agreement with the value of k<sub>obs</sub><sup>NO<sub>2</sub></sup> = 1.9 x 10<sup>-5</sup> s<sup>-1</sup> predicted from Figure 6 for decomposition of PAN at 25°C in the presence of 3.15 x 10<sup>-4</sup> M unlabeled NO<sub>2</sub>. However, in addition to the disappearance of total PAN, a much more rapid exchange reaction is occurring, which causes the simultaneous disappearance of



SA-4466-2

FIGURE 7 CONCENTRATION OF  $\text{NO}_2^*$  (○-○),  $\text{PAN} + \text{PAN}^*$  (●-●),  $\text{PAN}$  (▲-▲), AND  $\text{PAN}^*$  (○-○) VERSUS TIME FOR DECOMPOSITION OF  $0.78 \times 10^{-4} \text{M}$  PAN IN THE PRESENCE OF  $3.15 \times 10^{-4} \text{M}$   $^{15}\text{NO}_2$  AT  $25^\circ\text{C}$

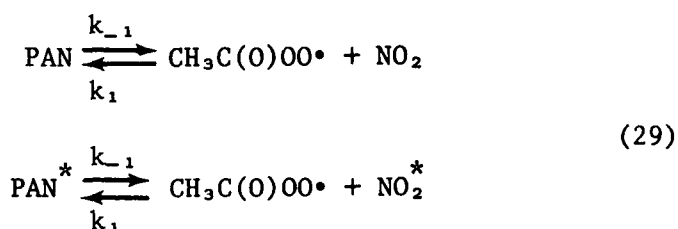
Table 3. SELECTED INFRARED ABSORPTION FREQUENCIES ( $\nu$ ) FOR PAN,  $^{15}\text{N}$ -LABELED PAN ( $\text{PAN}^*$ ),  $\text{NO}_2$ , AND  $^{15}\text{NO}_2$  ( $\text{NO}_2^*$ )

Compound	$\nu$ , $\text{cm}^{-1}$
PAN	1835, 1735
$\text{PAN}^*$	1835, 1696 <sup>a</sup>
$\text{NO}_2$	1618
$\text{NO}_2^*$	1590 <sup>b</sup>

<sup>a</sup>Reference 34.

<sup>b</sup>Reference 35.

PAN and  $\text{NO}_2^*$  and production of  $\text{PAN}^*$ . Though it is not shown in the figure,  $\text{NO}_2$  was produced at a rate parallel to that of  $\text{NO}_2^*$  disappearance. Clearly, this exchange can only result from the combination of acetylperoxy radicals (formed by reaction -1) with  $\text{NO}_2$  and  $\text{NO}_2^*$ :



Applying the steady-state approximation to the concentration of acetylperoxy radicals, the kinetic expression for the exchange reaction is:

$$\begin{aligned} +d[\text{PAN}^*]/dt &= -d[\text{NO}_2^*]/dt \\ &= k_{-1}\{([\text{PAN}] + [\text{PAN}^*])([\text{NO}_2^*]/[\text{NO}_2] + [\text{NO}_2^*]) - [\text{PAN}^*]\} \end{aligned} \quad (30)$$

Figure 7 shows that at any time,  $t$ , a tangent to the curve for  $\text{NO}_2^*$  disappearance has slope  $= (-d[\text{NO}_2^*]/dt)_t$ . Similarly, it is possible to directly determine the values  $[\text{PAN}^*]_t$  and  $([\text{PAN}] + [\text{PAN}^*])_t$ . As noted previously, it is difficult to measure  $[\text{NO}_2]$  accurately. Therefore, to

find the value for  $[\text{NO}_2^*]/([\text{NO}_2] + [\text{NO}_2^*])_t$ , it is assumed that the  $\text{NO}_2$  formed at any point in time equals the  $\text{NO}_2$  consumed, which gives:

$$[\text{NO}_2^*]/([\text{NO}_2] + [\text{NO}_2^*])_t = [\text{NO}_2^*]_t/[\text{NO}_2^*]_0 \quad (31)$$

Substituting equation 31 into equation 30 and rearranging gives:

$$k_{-1} = (-d[\text{NO}_2^*]/dt)_t \cdot \{([\text{PAN}] + [\text{PAN}^*])_t ([\text{NO}_2^*]_t/[\text{NO}_2^*]_0) - [\text{PAN}^*]_t\}^{-1} \quad (32)$$

Equation 32 and Figure 7 were used to calculate values for  $k_{-1}$  for six time points during the exchange reaction. Individual values of  $k_{-1}$ , the average of the six values, and the kinetic parameters used in the determinations are summarized in Table 4.

Table 4. KINETIC PARAMETERS FOR DECOMPOSITION OF  $0.78 \times 10^{-4}$  M PAN IN THE PRESENCE OF  $3.15 \times 10^{-4}$  M  $^{15}\text{NO}_2$  AT  $25^\circ\text{C}^a$

Time, s	$(-d[\text{NO}_2^*]/dt)_t$ $\text{M s}^{-1} \times 10^8$	$([\text{PAN}] + [\text{PAN}^*])_t \cdot$ $\left\{ \left( \frac{[\text{NO}_2^*]_t}{[\text{NO}_2^*]_0} \right) - [\text{PAN}^*]_t \right\}$	$k_{-1}^b$ $\text{s}^{-1} \times 10^4$
600	2.8	0.57	4.9
900	1.9	0.49	3.9
1200	1.3	0.42	3.1
1500	0.83	0.36	2.3
1800	0.58	0.32	1.8
2100	0.58	0.28	2.1
			average = $3.0 \pm 1.1$

<sup>a</sup>Date of Figure 7.

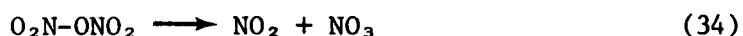
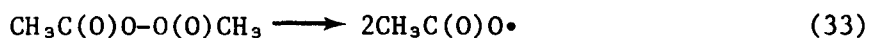
<sup>b</sup> $k_{-1}$  calculated from eq 32, see text.

The exchange experiment was repeated a total of nine times, and six individual values of  $k_{-1}$  were found for each experiment. The average value of all 54 individual rate constants is  $4.0 \pm 1.0 \times 10^{-4} \text{ s}^{-1}$ , in



excellent agreement with the value of  $k_{-1} = 3.7 \pm 0.39 \times 10^{-4} \text{ s}^{-1}$  obtained from the experiments with NO.<sup>36</sup> Because the decompositions in the presence of NO and NO<sub>2</sub><sup>\*</sup> proceed at the same rate, they must share a common rate determining step, and hence a common mechanism. Of the possible mechanisms considered for PAN homolysis only, equilibrium -1,1 can satisfactorily explain both the NO and the NO<sub>2</sub><sup>\*</sup> results. Thus, we consider the mechanism involving O-N bond cleavage to be valid. The NO<sub>2</sub>-enhanced decomposition is attributed to reactions 16 through 18, 27 and 28, which accompany the equilibrium 1,-1 under our reaction conditions.

To test the possibility that O-O homolysis (or any other reaction)<sup>37</sup> could also accompany O-N bond scission, we set as an upper limit for the rate of reaction 6 the rate constant for decomposition of PAN in the absence of added reactants. At 25°C, therefore, reaction 6 can constitute no more than 0.4% of the total pathway for PAN homolysis. To explain the preference for O-N relative to O-O cleavage in PAN homolysis, it is necessary to consider the changes in the enthalpies and entropies of reactions -1 and 6. Using established heats of formation when available and calculated values when necessary,<sup>24,38-41</sup> it is estimated that both reactions -1 and 6 are endothermic by the same amount,  $26 \pm 2 \text{ kcal/mol}^{-1}$ . This value is in good agreement with the activation energy determined experimentally for the PAN/NO system. Entropy changes for the two reactions are estimated to be  $\Delta S_{-1}^0 = 42 \pm 2$  and  $\Delta S_6^0 = 30 \pm 2 \text{ cal deg}^{-1} \text{ mol}^{-1}$  (1 atm standard state). To estimate the effect of the calculated entropy change on the rate of reaction 6, it is helpful to refer to rate data for acetyl peroxide and dinitrogen pentoxide homolyses (reactions 33 and 34):



For reactions 33 and 34, the entropy changes and Arrhenius pre-exponential factors are:<sup>42</sup>

$$\Delta S_{33}^0 = 33.4 \text{ cal deg}^{-1} \text{ mol}^{-1}, A_{33} = 10^{14.25} \text{ s}^{-1}$$

and

$$\Delta S_{34}^0 = 35.1 \text{ cal deg}^{-1} \text{ mol}^{-1}, A_{34} = 10^{14.78} \text{ s}^{-1}.$$

By analogy, the preexponential factor for reaction 6 is estimated to be  $A_6 = 10^{14} \text{ s}^{-1}$ . Because the preexponential factor for reaction -1,1 is observed to be  $A_{-1} = 10^{16.29} \text{ s}^{-1}$ , entropy effects could indeed dictate the 250-fold difference in the rate constants for reactions -1,1 and 6.

The calculated value for  $\Delta S_{-1}^0$  is useful in estimating  $k_1$ . If it is assumed that the radical-radical combination reaction (reaction 1) has zero activation energy, then

$$k_1 = A_1 \quad (35)$$

Also, from transition state theory,<sup>24</sup>

$$A_{-1}/A_1 = \exp(\Delta S_{-1}^0/R) \quad (36)$$

Therefore,  $\Delta S_{-1}^0$  (1 M standard states) and the observed value for  $A_{-1}$  can be used to calculate:

$$k_1 = A_{-1}/\exp(\Delta S_{-1}^0/R) = 1.0 \times 10^9 \text{ M}^{-1} \text{ s}^{-1}.$$

#### Decomposition of PAN in the Presence of NO and NO<sub>2</sub>

As discussed in the Introduction, the value for the rate constant  $k_1$  is important in terms of the atmospheric chemistry of peroxy radicals. Of equal importance is the value of  $k_2$ , the rate constant for reaction of peroxy radicals with NO. To determine a value of  $k_2$  for acetylperoxy radicals, we have measured the rate of decomposition of PAN in the presence of known concentrations of added NO and NO<sub>2</sub>.

In the PAN/NO/NO<sub>2</sub> system, equation 19 should apply. When NO and NO<sub>2</sub> are present in comparable amounts that exceed the amount of PAN, the disappearance of PAN should follow first-order kinetics. Defining  $k_{\text{obs}}^{\text{NO}_x}$  as the observed first-order rate constant for decomposition of PAN in the presence of added NO and NO<sub>2</sub>, equation 19 becomes

$$-d[\text{PAN}]/dt = [\text{PAN}]k_{-1}\{k_2[\text{NO}]/(k_2[\text{NO}] + k_1[\text{NO}_2])\} = [\text{PAN}]k_{\text{obs}}^{\text{NO}_x} \quad (37)$$

However, this treatment neglects the fact that NO<sub>2</sub> in excess of PAN enhances the rate of PAN decomposition. To correct for this empirically, we include a term for the NO<sub>2</sub>-enhanced decomposition in equation 37 to give:

$$[\text{PAN}]k_{\text{obs}}^{\text{NO}_x} = [\text{PAN}]k_{-1}\{k_2[\text{NO}]/(k_2[\text{NO}] + k_1[\text{NO}_2])\} + [\text{PAN}]k_{\text{obs}}^{\text{NO}_2} \quad (38)$$

Taking the reciprocal of equation 38 and rearranging gives:

$$(k_{\text{obs}}^{\text{NO}_x} - k_{\text{obs}}^{\text{NO}_2})^{-1} = (k_{-1})^{-1} + ([\text{NO}_2]/[\text{NO}])(k_1/k_2k_{-1}) \quad (39)$$

Thus, a plot of  $(k_{\text{obs}}^{\text{NO}_x} - k_{\text{obs}}^{\text{NO}_2})^{-1}$  versus  $[\text{NO}_2]/[\text{NO}]$  should be linear with slope =  $k_1/k_2k_{-1}$  and intercept =  $(k_{-1})^{-1}$ . To test the validity of equation 39, we measured PAN decomposition rates in the presence of excess NO and NO<sub>2</sub> at 25, 34.3, 39.0, and 43.9°C. Semilogarithmic plots of  $[\text{PAN}]_t/[\text{PAN}]_0$  versus time were typically linear to at least 50% decomposition, although upward curvature was sometimes noted for cases of low  $[\text{NO}]/[\text{NO}_2]$ . Linear regions of the semilogarithmic plots were used to obtain  $k_{\text{obs}}^{\text{NO}_x}$  values, and these are summarized in Table 5 along with reaction conditions and values of  $k_{\text{obs}}^{\text{NO}_2}$  for the experiments. For decompositions at 25, 34.3, and 43.9°C,  $k_{\text{obs}}^{\text{NO}_2}$  values were taken directly from Figure 6. For data at 39.0°C,  $k_{\text{obs}}^{\text{NO}_2}$  values were calculated from the relationship  $(k_{\text{obs}}^{\text{NO}_2})/[\text{NO}_2] = 0.49 \pm .04 \text{ M}^{-1} \text{ s}^{-1}$ . This relationship was obtained by interpolation of a plot (now shown) of  $\log(k_{\text{obs}}^{\text{NO}_2}/[\text{NO}_2])$  at a given temperature (i.e., the log of the slope of each line in Figure 6) versus

reciprocal absolute temperature. For the semilogarithmic plot, slope =  $4776 \pm 300$ , intercept =  $14.82 \pm 1.0 \text{ s}^{-1}$ , and correlation coefficient = 0.996.

Figure 8 is a plot of Table 5. The figure exhibits considerable scatter, probably because of inaccuracies in determining  $k_{\text{obs}}^{\text{NO}_2}$ . Nevertheless, the slopes and intercepts of the figure can be meaningfully used to calculate  $k_2/k_1$  ratios for each temperature. Least-squares data and the calculated ratios are given in Table 6. It is seen that  $k_2/k_1$  is essentially independent of temperature, which is to be expected for reactions 1 and 2, both of which should have negligible activation energies. The average value for the four ratios is  $k_2/k_1 = 3.02 \pm 0.68$ . This average is used to calculate  $k_2$  from the previously determined value of  $k_1$ . Thus,

$$k_2 = 3.02(1.0 \times 10^9 \text{ M}^{-1} \text{ s}^{-1}) = 3.0 \times 10^9 \text{ M}^{-1} \text{ s}^{-1}$$

which compares favorably with the value of  $5.0 \times 10^9 \text{ M}^{-1} \text{ s}^{-1}$  reported by Howard et al. for  $\text{HO}_2$  plus  $\text{NO}$ .<sup>43</sup>

## CONCLUSIONS

The equilibrium -1,1 between PAN, acetylperoxy radical, and  $\text{NO}_2$  has useful practical applications as well as some interesting environmental ramifications.

We find PAN to be a convenient thermal source of gas phase acetylperoxy radicals and  $\text{NO}_2$ . Low concentrations of PAN are easily prepared and safely handled, and the rate of O-N cleavage is rapid even at moderate temperatures ( $t_{1/2}$  for homolysis = 31 min at  $25^\circ\text{C}$ ). By observing the decomposition of PAN in the presence of a free radical scavenger, it is possible to measure the rate of reaction of acetylperoxy radicals with the scavenger relative to the rate of combination of acetylperoxy radicals with  $\text{NO}_2$  ( $k_1 = 1.0 \times 10^9 \text{ M}^{-1} \text{ s}^{-1}$ ). We have used this method to determine a value for the important reaction of acetylperoxy radicals with NO ( $k_2 = 3.0 \times 10^9 \text{ M}^{-1} \text{ s}^{-1}$ ). A study of the competition between acetylperoxy radicals,  $\text{NO}_2$ , and some hydrogen atom donors suggests that the

Table 5. RATE CONSTANTS AND REACTION CONDITIONS FOR DECOMPOSITION OF PAN  
IN THE PRESENCE OF ADDED NO AND NO<sub>2</sub> AT VARIOUS TEMPERATURES

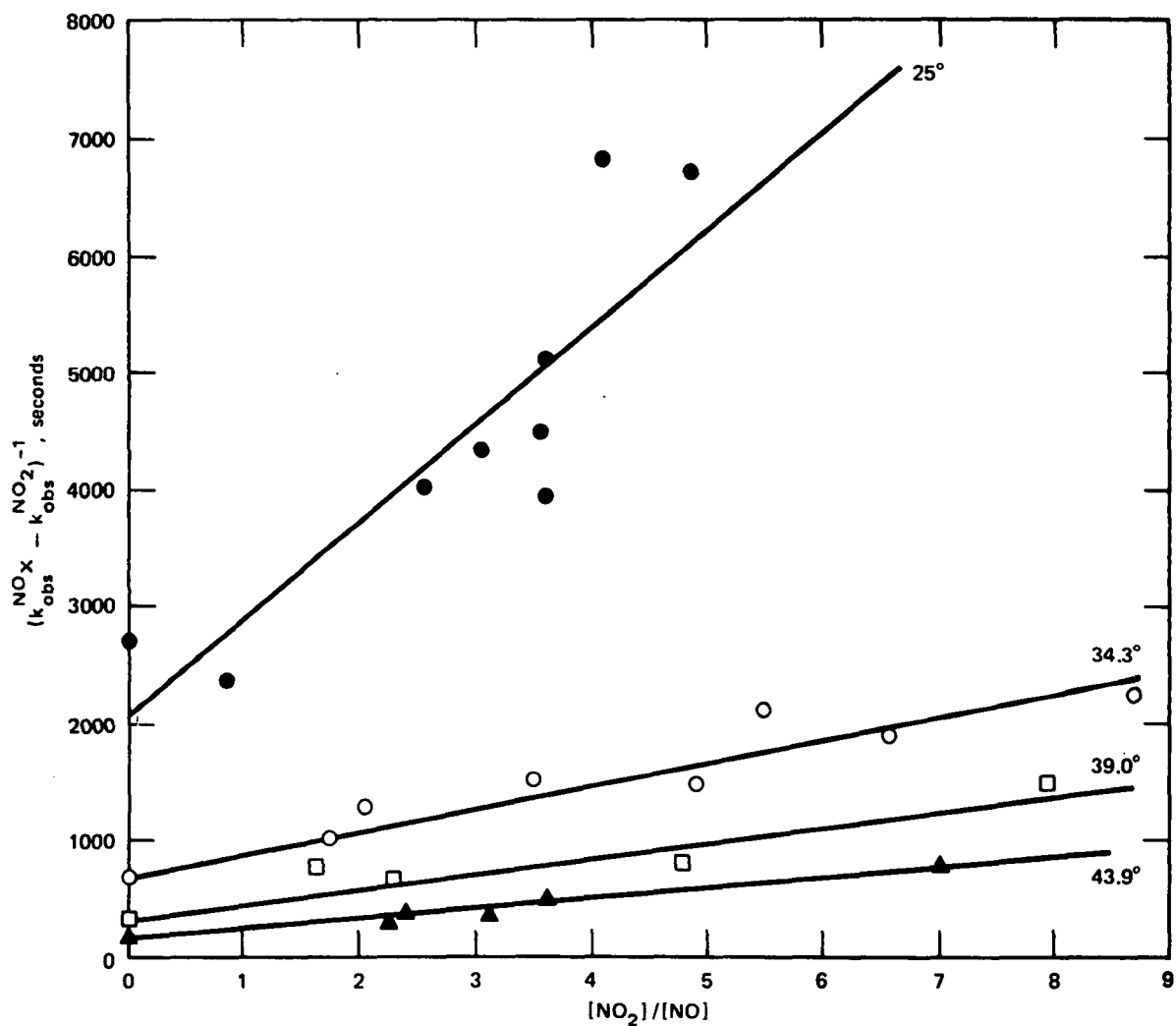
Temp °C	[PAN] M x 10 <sup>4</sup>	[NO <sub>2</sub> ]/[NO]	[NO <sub>2</sub> ] M x 10 <sup>4</sup>	k <sub>obs</sub> <sup>NO<sub>2</sub></sup> <sup>a</sup> s <sup>-1</sup> x 10 <sup>4</sup>	k <sub>obs</sub> <sup>NOx</sup> <sup>b</sup> s <sup>-1</sup> x 10 <sup>4</sup>	(k <sub>obs</sub> <sup>NOx</sup> - k <sub>obs</sub> <sup>NO<sub>2</sub></sup> ) <sup>-1</sup> s x 10 <sup>-3</sup>
25	-		0	0	3.7 <sup>c</sup>	2.70
	0.730	0.83	4.10	0.25	4.48	2.36
	0.746	2.56	5.47	0.33	2.82	4.01
	1.03	3.03	2.79	0.17	2.49	4.31
	0.645	3.54	3.54	0.32	2.57	4.45
	0.948	3.59	4.32	0.26	2.83	3.90
	0.799	3.59	6.03	0.36	2.32	5.11
	0.572	4.08	5.22	0.31	1.79	6.77
	1.33	4.85	3.05	0.18	1.68	6.68
34.3	-	0	0	0	14.0 <sup>c</sup>	0.714
	0.823	1.70	3.02	0.51	10.5	1.00
	1.01	2.03	3.83	0.56	8.45	1.28
	0.537	3.45	3.43	0.58	7.10	1.53
	1.32	4.85	6.86	1.17	7.86	1.49
	0.830	5.40	4.70	0.80	5.56	2.10
	0.941	6.53	6.22	1.06	6.34	1.89
	0.651	8.67	5.59	0.95	5.39	2.25
39.0	-	0	0	0	29.0 <sup>c</sup>	0.345
	0.996	1.62	3.73	1.68	13.6	0.840
	0.601	2.25	3.88	1.66	16.3	0.683
	1.83	4.75	3.35	1.51	13.7	0.820
	0.971	7.93	5.21	2.34	9.11	1.48
43.9	-	0	0	0	52.2 <sup>d</sup>	0.192
	0.488	2.25	2.69	1.48	33.5	0.310
	0.562	2.31	4.47	2.46	28.5	0.384
	0.858	3.09	2.34	1.29	28.1	0.373
	0.922	3.63	3.02	1.66	21.1	0.514
	0.848	7.00	3.38	1.86	14.3	0.804

<sup>a</sup>From linear region of semilogarithmic plot of [PAN]<sub>t</sub>/[PAN]<sub>0</sub> versus time

<sup>b</sup>From Figure 6, except for 39.0° data, in which case k<sub>obs</sub><sup>NO<sub>2</sub></sup> = 0.49[NO<sub>2</sub>]

<sup>c</sup>k<sub>obs</sub><sup>NO</sup> for [NO<sub>2</sub>]/[NO] = 0 is taken from k<sub>-1</sub> values of Table II

<sup>d</sup>k<sub>obs</sub><sup>NO</sup> for [NO<sub>2</sub>]/[NO] = 0 is taken from k<sub>-1</sub> value extrapolated from Figure 3.



SA-4466-8

FIGURE 8 RECIPROCAL CORRECTED RATE CONSTANT  $(k_{\text{obs}}^{\text{NO}_x} - k_{\text{obs}}^{\text{NO}_2})^{-1}$  VERSUS  $[\text{NO}_2]/[\text{NO}]$  FOR DECOMPOSITION OF PAN IN THE PRESENCE OF ADDED  $\text{NO}_2$  AND  $\text{NO}$  AT; 25°C (●-●), 34.3°C (○-○), 39.0°C (□-□), AND 43.9°C (▲-▲)

Table 6. LEAST SQUARES DATA FOR FIGURE 8 AND CALCULATED VALUES OF  $k_2/k_1$  FOR DECOMPOSITION OF PAN IN THE PRESENCE OF ADDED  $\text{NO}_2$  AND  $\text{NO}$  AT VARIOUS TEMPERATURES

Temp °C	Slope <sup>a</sup> s x 10 <sup>-3</sup>	Intercept <sup>a</sup> s x 10 <sup>-3</sup>	r <sup>2</sup>	(k <sub>-1</sub> ) <sup>-1</sup> s x 10 <sup>-3</sup>	k <sub>2</sub> /k <sub>1</sub> <sup>d</sup>
25.0	0.861 ± 0.177	1.48 ± 0.58	0.768	2.70 <sup>b</sup>	3.14
34.3	0.178 ± 0.025	0.807 ± 0.119	0.897	0.714 <sup>b</sup>	4.01
39.0	0.123 ± 0.029	0.425 ± 0.124	0.860	0.345 <sup>b</sup>	2.80
43.9	0.900 ± 0.034	0.155 ± 0.009	0.959	0.192 <sup>c</sup>	2.13

<sup>a</sup>Error limits are standard deviations

<sup>b</sup>k<sub>-1</sub> taken from Table 2

<sup>c</sup>k<sub>-1</sub> extrapolated from Figure 3.

<sup>d</sup>k<sub>2</sub>/k<sub>1</sub> = (slope x k<sub>-1</sub>)<sup>-1</sup>, see eq 39.

technique can be applied to the reaction of acetylperoxy radicals with a wide variety of organic substrates.

Environmentally, PAN has until now been considered a product of photochemical smog only. The equilibrium -1,1, however, suggests that PAN may also have a significant effect in causing the formation of air pollution. Under ambient conditions of high  $\text{NO}_2/\text{NO}$  (such as in late afternoon or at night), PAN accumulates and persists in the environment. However, when the ambient level of  $\text{NO}$  increases (e.g., when exhaust emissions increase in early morning) PAN decomposes rapidly, resulting in the oxidation of  $\text{NO}$  to  $\text{NO}_2$ . Computer simulation of the propylene/ $\text{NO}_x$ <sup>44</sup> system indicates that including the equilibrium -1,1 in the model increases both the initial rate of ozone products and the maximum level of ozone produced. Thus, PAN may play an important role in the early morning chemistry of polluted atmospheres.

Contrary to suggestions in the literature<sup>45,46</sup> the thermochemistry of the mechanism of homolysis of peroxy nitrates in general indicates

that O-N cleavage should predominate over O-O homolysis for  $\text{ROONO}_2$ , where R is H, alkyl, acyl, and aroyl.

Finally, we compare our values of  $k_2/k_1 = 3.02 \pm 0.68$  and  $k_1 = 10^{(16.29 \pm 0.60)} \exp(26910 \pm 900/\theta) \text{ s}^{-1}$  to values for these rate constants that have been reported by Cox and Roffey.<sup>47</sup> From a study of the rate of oxidation of NO to  $\text{NO}_2$  by PAN, these authors found  $k_2/k_1 = 1.85 \pm 0.6$  and  $k_{-1} = 10^{(14.90 \pm 0.60)} \exp(24860 \pm 760/\theta) \text{ s}^{-1}$ . The two expressions of  $k_{-1}$  give identical values at 322K, while at 300K the calculated value of Cox and Roffey is 27% of our calculated value. We believe our values are to be preferred because our method involves direct measurements of PAN, whereas Cox and Roffey actually measured changes in NO concentration. The latter method requires knowing the number of NO molecules oxidized per molecule of PAN decomposed, and there is some uncertainty in the determination of this quantity using Cox and Roffey's method.



#### 4. GAS PHASE HYDROXYL RADICAL REACTIONS. PRODUCTS AND PATHWAYS

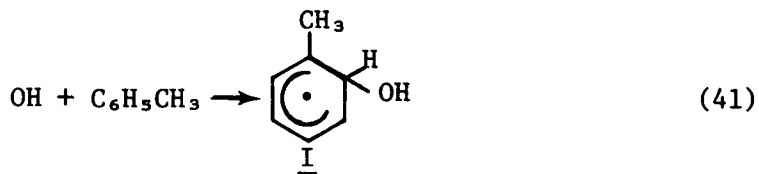
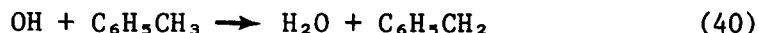
##### FOR THE REACTION OF OH WITH AROMATIC HYDROCARBONS

###### INTRODUCTION

Aromatic hydrocarbons are important constituents of polluted urban atmospheres<sup>48</sup> and the extent to which they contribute to photochemical smog is of considerable concern.<sup>49-52</sup> Their participation in atmospheric chemistry is the result of reaction with OH radical. The kinetics of gas phase OH-aromatic reactions have been the subject of several recent reports,<sup>53-58</sup> and it is clear that initial attack by OH is the major route for involvement of aromatic hydrocarbons in the chemistry of the troposphere.<sup>59,60</sup> Although the mechanisms of solution phase OH-alkyl benzene reactions have been extensively investigated,<sup>61-68</sup> reactions in the gas phase, where ambiguities due to solvation or solvolysis are excluded, have not been studied in depth. Thus products and precise mechanisms of the gas phase reactions remain undetermined; however, identifying them is essential for determining the fate of aromatics in the environment and for developing accurate chemical models of urban airsheds.

Given these considerations, we have undertaken to determine directly the products of the gas phase reaction of OH with benzene, toluene, p-xylene, and 1,3,5-trimethylbenzene.

Our results show that two major reaction pathways are available. Shown for the case of toluene, these are benzylic hydrogen atom abstraction (reaction 40) and radical addition to the aromatic ring (reaction 41).



For each of the hydrocarbons studied, we have determined the relative incidence of reaction 40 and reaction 41 by product analyses. Our data are in close agreement with relative rate constants determined by kinetic experiments.<sup>58</sup> The intramolecular selectivity of ring addition to toluene by OH is also reported and discussed in terms of formation of an intermediate OH-toluene  $\pi$ -complex. Finally, we consider the environmental implications of our findings.

## EXPERIMENTAL SECTION

### Materials

The benzene and toluene used were Malinckrodt Analytical Reagent grade. 1,4-Dimethylbenzene (99%) and 1,3,5-trimethylbenzene (99+%, Gold Label) were from Aldrich Chemical Company. Benzene, toluene, and 1,4-dimethylbenzene were purified by reaction with concentrated  $\text{H}_2\text{SO}_4$ , phase separation, three aqueous washings, drying with  $\text{MgSO}_4$ , and fractional distillation. 1,3,5-Trimethylbenzene was fractionally distilled before use. Argon,  $\text{H}_2$ , and  $\text{O}_2$  were supplied by Liquid Carbonics and  $\text{NO}_2$  (0.54% in He) by Linde.

### Apparatus

The flow system used in the studies was constructed of 2.5 cm i.d. Pyrex tubing. O-ring joints and stopcocks with Viton o-rings were used throughout. A Scintillonics model HVI5A generator was used to produce the microwave discharge. A power level of 50 w was typically employed. Pressures of gaseous reactants were measured with a Validyne model DP7 Transducer. The main pump was an Alcatel direct-drive model.

Glpc analyses were performed with a Hewlett-Packard model 5700A chromatograph equipped with a flame-ionization detector. A Finnigan Model 3200 tandem GC-MS was used for product identification. Hplc analyses were performed with a Waters Associates system consisting of two model 6000A pumps, a model 660 solvent programmer, and a U6K injector. A Schoeffel Instrument Corporation model GM770 variable wave-length detector was used.

## Methods

### Reaction Conditions

Aromatic hydrocarbons were added by syringe at a rate of  $0.17 \text{ cm}^3 \text{ min}^{-1}$  maintained by a syringe pump. Hydrogen atoms were generated by passing a dilute mixture of  $\text{H}_2$  in Ar through the microwave discharge. Typical reactant pressures (torr) were:  $\text{H}_2$ , 0.2; Ar, 5; hydrocarbon, 0.1;  $\text{NO}_2$ ,  $1 \text{ to } 5 \times 10^{-3}$ ; He, 0.2 to 1;  $\text{O}_2$ , 1 to 10. Total pressures thus ranged from 6 to 15 torr. The linear flow velocity of the system was  $1.0 \times 10^3 \text{ cm s}^{-1}$ . All reactions were carried out at ambient temperature,  $25 \pm 3^\circ\text{C}$ .

### Product Analysis

Products were sampled by condensation in a cold trap ( $-78$  or  $-196^\circ\text{C}$ ) or by pulling a fraction of the gas stream through a short glpc column packed with Chromosorb G, AW/DMCS, 100/120 mesh (Applied Science). Control experiments demonstrated that the condensation traps collected only about 10% of the organic material passing through the system. For this reason, mass balances could not be obtained. Other experiments showed, however, that condensable species were trapped nonselectively, i.e., that product ratios in the condensed material were equivalent to ratios in the gas stream. Control experiments to test the efficiency of the gas sampling system showed that products were not quantitatively trapped on the Chromosorb G column, the more volatile materials being pulled through the column to the sampling pump. Gas sampling could therefore be used only for qualitative analysis.

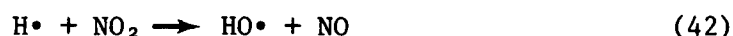
Product distributions from both condensed and gas phase sampling methods were carefully compared to rule out the possibility of interference caused by side reactions occurring in the cold trap.<sup>69</sup>

Products were identified by GC-MS and by comparing glpc retention times with authentic samples. Toluene and its reaction products were analyzed using a  $2.5 \text{ m} \times 0.5 \text{ mm}$  ID stainless steel column packed with 4% tri-2-cresylphosphate on 100/120 mesh Chromosorb G AW/DMCS and a  $1.8 \text{ m} \times 1.0 \text{ mm}$  glass column packed with 10% OV-17 on 80/100 mesh Chromosorb W. Benzene and

its reaction products were analyzed with the same OV-17 column. The tri-cresylphosphate column was also used for analysis of 1,4-dimethyl benzene and 1,3,5-trimethylbenzene reactions. Products of the latter reaction were also analyzed by hplc using a  $\mu$ -Bondapak C<sub>18</sub> column with 30% CH<sub>3</sub>CH/H<sub>2</sub>O as the mobile phase. Glpc and hplc response factors were obtained for all products.

## RESULTS

Hydroxyl radicals were generated by the discharge flow method from hydrogen atoms and NO<sub>2</sub>,



This method has been used extensively<sup>70-76</sup> for determination of OH reaction kinetics and is known to be reliable. In our system, an aromatic hydrocarbon and molecular oxygen are added 10 cm downstream from the point of addition of NO<sub>2</sub>. For the linear flow velocity ( $1.0 \times 10^3 \text{ cm s}^{-1}$ ) and concentrations of hydrogen atoms, and NO<sub>2</sub> ( $[\text{H}\cdot] \approx 6 \times 10^{13} \text{ particles cm}^{-3}$ )<sup>77</sup> used in our system, reaction 42 ( $k_{12} = 4.8 \times 10^{-11} \text{ cm}^3 \text{ molec}^{-1} \text{ s}^{-1}$ )<sup>78</sup> has gone to completion at this point. Providing that the amount of [NO<sub>2</sub>] added is greater than or equal to the amount of [H•], the products observed will have resulted entirely from reaction of OH with the aromatic hydrocarbon in the presence of O<sub>2</sub>, NO° and NO<sub>2</sub>. When a hydrocarbon concentration [ $3 \times 10^{15} \text{ molecule cm}^{-3}$ ] higher than the concentration of OH [ $\approx 10^{12} \text{ particles cm}^{-3}$ ]<sup>30</sup> is maintained, conversion is low and secondary OH-aromatic reactions are negligible.

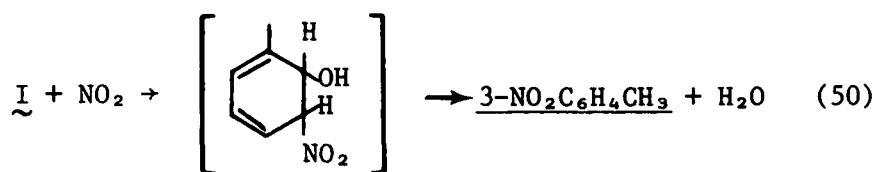
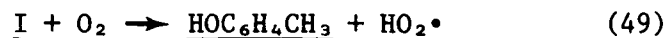
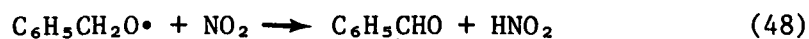
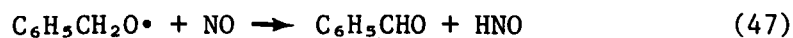
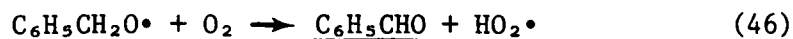
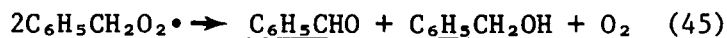
The gas phase products of the reaction of OH with toluene were found to be benzaldehyde (C<sub>6</sub>H<sub>5</sub>CHO), benzyl alcohol (C<sub>6</sub>H<sub>5</sub>CH<sub>2</sub>OH), 3-nitrotoluene (3-NO<sub>2</sub>C<sub>6</sub>H<sub>4</sub>CH<sub>3</sub>), isomeric cresols (2-, 3-, 4-HOC<sub>6</sub>H<sub>4</sub>CH<sub>3</sub>), and 2-methyl-1,4-benzoquinone (CH<sub>3</sub>C<sub>6</sub>H<sub>3</sub>O<sub>2</sub>). Phenol, benzoic acid, benzyl nitrate, and  $\alpha$ -, 2-, and 4-nitrotoluene were searched for but not found. We set 1% of the total reaction products as an upper limit for the formation of each of these products. In some runs, small (< 1% of the total products) amounts of an unidentified product less retentive on glpc than toluene were also observed.

Similar results were obtained with hydrocarbons other than toluene. Reaction of OH with benzene yielded phenol and nitrobenzene. The reaction with 1,4-dimethylbenzene gave 4-CH<sub>3</sub>C<sub>6</sub>H<sub>4</sub>CHO, 4-CH<sub>3</sub>C<sub>6</sub>H<sub>4</sub>CH<sub>2</sub>OH, 2-HO-1,4-(CH<sub>3</sub>)<sub>2</sub>C<sub>6</sub>H<sub>3</sub>, and 2-NO<sub>2</sub>-1,4-(CH<sub>3</sub>)<sub>2</sub>C<sub>6</sub>H<sub>3</sub>. Finally, the products of reaction of OH with 1,3,5-trimethylbenzene were 3,5-(CH<sub>3</sub>)<sub>2</sub>C<sub>6</sub>H<sub>3</sub>CHO, 3,5-(CH<sub>3</sub>)<sub>2</sub>C<sub>6</sub>H<sub>3</sub>CH<sub>2</sub>OH, and 2-HO-1,3,5-(CH<sub>3</sub>)<sub>3</sub>C<sub>6</sub>H<sub>2</sub>.

For each hydrocarbon, product distributions were studied quantitatively as a function of [O<sub>2</sub>], [NO<sub>2</sub>], and total pressure. These experiments were studied in greatest detail for the case of toluene. Product distributions for this reaction at constant [O<sub>2</sub>] and various [NO<sub>2</sub>] are given in Table 7. Table 8 gives distributions at constant [NO<sub>2</sub>] as a function of [O<sub>2</sub>] and total pressure.

## DISCUSSION

Tables 7 and 8 show that the individual product yields vary with reaction conditions, but the ratio (C<sub>6</sub>H<sub>5</sub>CHO + C<sub>6</sub>H<sub>5</sub>CH<sub>2</sub>OH)/(total products) is independent of NO<sub>2</sub>, O<sub>2</sub>, and total pressure. A mechanism that accounts for this and for the observed products of all the OH-aromatic reactions is given (for the case of toluene) by reactions 40-51:





Reactions 43 through 48 are analogous to the known reactions of methyl,<sup>79</sup> methylperoxy,<sup>80,81</sup> and methoxy<sup>82,83</sup> radicals. Reaction 49 closely resembles the reaction of cyclohexadienyl radicals with O<sub>2</sub>.<sup>84</sup> Reaction 50<sup>85</sup> and similar addition-elimination reactions<sup>86,87</sup> have been observed in solution. Reaction 51 has been the subject of numerous recent investigations.<sup>88-91</sup>

According to the proposed mechanism, C<sub>6</sub>H<sub>5</sub>CHO and C<sub>6</sub>H<sub>5</sub>CH<sub>2</sub>OH result ultimately from benzylic hydrogen atom abstraction (reaction 40), whereas 3-nitrotoluene and cresols result from ring addition (reaction 41). Thus the ratio of abstraction products to total products should be a constant governed by the ratio  $k_{40}/(k_{40} + k_{41})$ . We have run the HO-toluene reaction a total of 20 times, and for all runs the average value of (C<sub>6</sub>H<sub>5</sub>CHO + C<sub>6</sub>H<sub>5</sub>CH<sub>2</sub>OH) / (total products) was  $0.15 \pm 0.02$ . This is in excellent agreement with the value of  $k_{40}/(k_{40} + k_{41}) = 0.14^{+0.07}_{-0.05}$  obtained by Perry et al.<sup>58</sup> using a flash photolysis-resonance fluorescence technique. Values of  $k_{40}/(k_{40} + k_{41})$  were calculated for the other hydrocarbons used in our study. As Table 9 shows, our values of  $k_{40}/(k_{40} + k_{41})$  agree in all cases with those of Perry et al. within the limits of experimental uncertainty.

Over the pressure range of our experiments, we have found no evidence of a pressure effect. Therefore we believe that the reversible decomposition of the hot OH-aromatic adducts is not occurring in our system. This is supported by earlier work of Davis et al.<sup>55</sup> For the case of toluene, these workers found that at 298 K and 5 to 15 torr of He bath gas, the value of  $(k_{40} + k_{41})$  was about 0.8 of the high pressure value. Since our results were obtained with a mixture of Ar and O<sub>2</sub> as bath gas rather than He, our value of  $k_{40}/(k_{40} + k_{41})$  is expected to be essentially at the high pressure limit. Variations in  $k_{40}/(k_{40} + k_{41})$  over the pressure range 6 to 15 torr should be well within the  $\pm 13\%$  standard deviation observed for our experiments with toluene. Reaction  $k_{41}$  for the dimethyl- and trimethylbenzenes should be even

Table 7. DISTRIBUTION OF INDIVIDUAL PRODUCTS AS A FUNCTION OF  $[\text{NO}_2]$  ADDED FOR REACTION OF OH WITH TOLUENE PLUS  $9.7 \times 10^{16}$  MOLEC  $\text{CM}^{-3}$   $\text{O}_2^a$

$[\text{NO}_2]$ molec $\text{cm}^{-3}$ $\times 10^{-14}$	Individual Product as % of Total							$\text{CH}_3\text{C}_6\text{H}_4\text{O}_2$	$\text{C}_6\text{H}_5\text{CHO} + \text{C}_6\text{H}_5\text{CH}_2\text{OH}$ Total	Total Products $\text{C}_6\text{H}_5\text{CH}_3$ $\times 10^4$
	$\text{C}_6\text{H}_5\text{CHO}$	$\text{C}_6\text{H}_5\text{CH}_2\text{OH}$	$3\text{-NO}_2\text{C}_6\text{H}_4\text{CH}_3$	$2\text{-HOC}_6\text{H}_4\text{CH}_3$	$4\text{-HOC}_6\text{H}_4\text{CH}_3$	$3\text{-HOC}_6\text{H}_4\text{CH}_3$	Total $\text{HOC}_6\text{H}_4\text{CH}_3$			
0.71	12.5	4.0	36.6	37.6	5.69	3.6	46.9	--	16.46	2.2
1.04	12.5	4.8	36.9	35.3	6.03	4.04	45.4	0.46	17.3	5.7
1.39	12.4	4.4	45.3	27.0	5.5	4.5	37.0	0.9	16.7	2.0
1.75	8.16	9.52	53.2	19.61	4.72	4.1	28.43	0.69	17.7	1.3

<sup>a</sup>Total pressure = 8.18 torr.

Table 8. DISTRIBUTION OF INDIVIDUAL PRODUCTS AS A FUNCTION OF  $[\text{O}_2]$  ADDED AND (F TOTAL PRESSURE FOR REACTION OF OH WITH TOLUENE USING  $1.39 \times 10^{16}$  MOLEC  $\text{CM}^{-3}$  ADDED  $\text{NO}_2$

$[\text{O}_2]$ molec $\text{cm}^{-3}$ $\times 10^{-16}$	Total Pressure, torr	Individual Product as % of Total							$\text{C}_6\text{H}_5\text{CHO} + \text{C}_6\text{H}_5\text{CH}_2\text{OH}$ (Total Products)	Total Products $\text{C}_6\text{H}_5\text{CH}_3$ $\times 10^4$
		$\text{C}_6\text{H}_5\text{CHO}$	$\text{C}_6\text{H}_5\text{CH}_2\text{OH}$	$3\text{-NO}_2\text{C}_6\text{H}_4\text{CH}_3$	$2\text{-HOC}_6\text{H}_4\text{CH}_3$	$3\text{-HOC}_6\text{H}_4\text{CH}_3$	$4\text{-HOC}_6\text{H}_4\text{CH}_3$	$\text{HOC}_6\text{H}_4\text{CH}_3$		
3.2	6.8	6.6	6.2	44.8	35.2	3.8	3.5	42.5	< 0.5	9.4
6.5	7.8	7.4	5.0	42.0	34.6	6.3	4.5	45.4	< 0.5	6.4
9.7	8.8	8.5	3.7	44.3	30.7	5.5	4.7	40.9	2.5	15.7
13.0	9.8	10.1	3.3	49.9	25.8	5.3	5.3	36.4	< 0.5	2.5
14.6	10.3	11.0	2.6	47.6	27.0	5.8	5.9	38.7	< 0.5	2.2
16.2	10.8	8.5	3.8	44.3	29.2	6.5	6.5	42.0	1.1	1.8
19.2	11.8	12.4	4.4	45.3	27.0	5.5	4.5	37.0	0.9	2.0

Table 9. PRODUCTS AND RATE CONSTANT RATIOS  $[k_1/(k_1 + k_2)]$  FOR REACTIONS OF OH WITH VARIOUS HYDROCARBONS IN THE PRESENCE OF  $\text{NO}_2$  AND  $\text{O}_2^a$

Hydrocarbon	Products	$k_{40}/(k_{40} + k_{41})$	
		This Work	Reference 58
benzene	$\text{C}_6\text{H}_5\text{OH}$ , $\text{C}_6\text{H}_5\text{NO}_2$	$< 0.05^b$	0.05 (0.01 to 0.13) <sup>c</sup>
toluene	$\text{C}_6\text{H}_5\text{CHO}^d$ , $\text{C}_6\text{H}_5\text{CH}_2\text{OH}^d$ , $\text{CH}_3\text{C}_6\text{H}_3\text{O}_2^e$ 3- $\text{NO}_2\text{C}_6\text{H}_4\text{CH}_3$ , 2,3, and 4- $\text{HOC}_6\text{H}_4\text{CH}_3$ ,	$0.15 \pm 0.02$	0.16 (0.11 - 0.23)
of 1,4-dimethylbenzene	4- $\text{CH}_3\text{C}_6\text{H}_4\text{CHO}^d$ , 4- $\text{CH}_3\text{C}_6\text{H}_4\text{CH}_2\text{OH}^d$ 2-HO-1,4- $(\text{CH}_3)_2\text{C}_6\text{H}_3$ 2- $\text{NO}_2$ -1,4- $(\text{CH}_3)_2\text{C}_6\text{H}_3$	$0.15 \pm 0.02$	0.07 (0.04 to 0.14)
1,3,5-trimethylbenzene	3,5- $(\text{CH}_3)_2\text{C}_6\text{H}_3\text{CHO}^d$ 3,5- $(\text{CH}_3)_2\text{C}_6\text{H}_3\text{CH}_2\text{OH}^d$ 2-HO-1,3,5- $(\text{CH}_3)_3\text{C}_6\text{H}_2$	$0.021 \pm 0.006$	0.02 0.01 to 0.06

<sup>a</sup>Reaction conditions employed were similar in all cases to those reported in Tables 7 and 8 for toluene.

<sup>b</sup>Represents fraction of total reaction proceeding by ring hydrogen atom abstraction.

<sup>c</sup>Values in parentheses represent the reported range.

<sup>d</sup>Products derived from benzylic hydrogen atom abstraction.

<sup>e</sup>Minor product.



less susceptible to reversibility than it is for toluene, and  $k_{41}$  occurs to the exclusion of other reactions for the case of benzene. We therefore conclude that the reverse of reaction 41 is unimportant at the temperature and pressures used in our experiments.

At this point we can calculate  $k_{41(o)}/k_{41}$ ,  $k_{41(m)}/k_{41}$ , and  $k_{41(p)}/k_{41}$  (for toluene) i.e., the portions of reaction 41 that proceed by OH attack at the 2-, 3-, and 4-positions, respectively. To derive these relative rate constants, we use the measured product ratios for 3-nitrotoluene and the isomeric cresols and the following relations:

$$k_{41(m)}/k_{41} = (3\text{-HOC}_6\text{H}_4\text{CH}_3)(\text{total cresols} + 3\text{-NO}_2\text{C}_6\text{H}_4\text{CH}_3)^{-1} \quad (52)$$

$$k_{41(o)}/k_{41} = \{[2\text{-HOC}_6\text{H}_4\text{CH}_3/(2\text{-HOC}_6\text{H}_4\text{CH}_3 + 4\text{-HOC}_6\text{H}_4\text{CH}_3)](3\text{-NO}_2\text{C}_6\text{H}_4\text{CH}_3) + 2\text{-HOC}_6\text{H}_4\text{CH}_3\}(\text{total cresols} + 3\text{-NO}_2\text{C}_6\text{H}_4\text{CH}_3)^{-1} \quad (53)$$

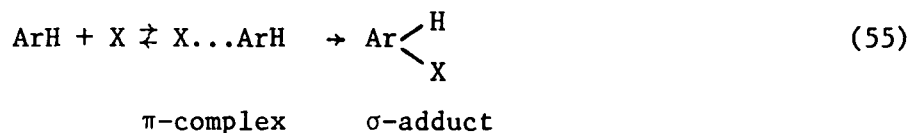
$$k_{41(p)}/k_{41} = \{[4\text{-HOC}_6\text{H}_4\text{CH}_3/(2\text{-HOC}_6\text{H}_4\text{CH}_3 + 4\text{-HOC}_6\text{H}_4\text{CH}_3)](3\text{-NO}_2\text{C}_6\text{H}_4\text{CH}_3) + 4\text{-HOC}_6\text{H}_4\text{CH}_3\}(\text{total cresols} + 3\text{-NO}_2\text{C}_6\text{H}_4\text{CH}_3)^{-1} \quad (54)$$

To derive equation 52, we recall that 2- and 4- $\text{NO}_2\text{C}_6\text{H}_4\text{CH}_3$  are not found as products and that 3- $\text{HOC}_6\text{H}_4\text{CH}_3$  is the only observed product derived from OH attack at the 3-position. For equations 52 and 54, we note that 3- $\text{NO}_2\text{C}_6\text{H}_4\text{CH}_3$  results from attack by OH at either the 2- or 4-position and assume that  $k_{11}$  is independent of the position of OH in the intermediate, I. In this case the total amount of product derived from OH attack ortho to the methyl group is equal to the observed amount of 2- $\text{HOC}_6\text{H}_4\text{CH}_3$  plus the fraction of the 3- $\text{NO}_2\text{C}_6\text{H}_4\text{CH}_3$  that was derived from I with OH in the 2-position, this fraction being equated to the product ratio

$$2\text{-HOC}_6\text{H}_4\text{CH}_3/(2\text{-HOC}_6\text{H}_4\text{CH}_3 + 4\text{-HOC}_6\text{H}_4\text{CH}_3) \quad .$$

For toluene, the average values of  $k_{41(o)}/k_{41}$ ,  $k_{41(m)}/k_{41}$ , and  $k_{41(p)}/k_{41}$  were:  $0.806 \pm 0.022$ ,  $0.051 \pm 0.009$ , and  $0.143 \pm 0.019$ , respectively. These values are compared in Table 10 to values obtained for addition of OH to

toluene in solution and for addition to toluene by other highly reactive species. From Table 10 it is evident that, in reactions with toluene, gas phase OH is at once a highly reactive and highly selective species. A similar parallel between reactivity and selectivity has been noted in some ionic electrophilic aromatic substitution reactions, and Olah<sup>94</sup> has suggested that a  $\pi$ -complex is involved in these reactions as a precursor to the formation of a  $\sigma$ -adduct:



The intermediacy of  $\pi$ -complexes in other radical reactions has been suggested, and, indeed, the formation of an OH-aromatic  $\pi$ -complex was considered by Perry et al as a possible explanation for the reversibility of reaction 41 under the conditions of their experiments. Although it is not conclusive, our evidence concerning the selectivity of the addition of OH to toluene lends credence to the postulated participation of  $\pi$ -complexes in OH-aromatic reactions. Regardless of the precise mechanism of the reaction, it is apparent that ortho-attack by OH is highly preferred for the addition to toluene. This behavior confirms<sup>64,96</sup> the electrophilic nature of the hydroxyl radical. That ortho attack by OH occurs more readily in the gas phase than in solution is attributable to steric effects that are significant for solvated OH but not for the free radical in the gas phase.

Next we wish to estimate the rate constant ratio  $k_{50}/k_{49}$ , i.e., the relative reactivities of  $\text{NO}_2$  and  $\text{O}_2$  toward the adduct I. To do this, we combine and integrate the kinetic expressions for reactions 49 and 50, giving:

$$k_{50}/k_{49} = \frac{(3\text{-NO}_2\text{C}_6\text{H}_4\text{CH}_3)}{(\text{total HOC}_6\text{H}_4\text{CH}_3)} \cdot \frac{[\text{O}_2]}{[\text{NO}_2]} \quad (56)$$

With our experimental method, the values for  $(3\text{-NO}_2\text{C}_6\text{H}_4\text{CH}_3)/(\text{total HOC}_6\text{H}_4\text{CH}_3)$  and  $[\text{O}_2]$  are readily determined, but the value for  $[\text{NO}_2]$  is not. The difficulty with  $[\text{NO}_2]$  is that a fraction of the added  $\text{NO}_2$  consumed in titrating  $\text{H}\cdot$  through reaction 42 and that there is no direct measure of  $[\text{H}\cdot]$  in our system. To

Table 10. REACTIVITY AND POSITIONAL SELECTIVITY OF RING-ADDITION TO TOLUENE BY VARIOUS SPECIES

Species	Phase	$k_{\text{add}}$ $\text{cm}^3 \text{ molecule}^{-1} \text{ sec}^{-1}$	100 x Fraction of Ring-Addition			References	
			2-Position	3-Position	4-Position	$k_{\text{add}}$	Products
OH	gas	$5.4 \times 10^{-12}$	80.6	5.1	14.3	19	this work
OH	soln(PhCH <sub>3</sub> )	--	59	6	35	--	8
OH	soln(H <sub>2</sub> O)	$4.8 \times 10^{-12}$	55	15	29.5	1	6
O( <sup>3</sup> P)	gas	$2.3 \times 10^{-13}$	60	15	18	93	92

estimate the  $[\text{NO}_2]$  in our system, we have developed a detailed kinetic model for the OH-toluene reaction and have used  $[\text{H}\cdot]$  as a variable to obtain a best fit of the model to the experimental data in a given run. Once an optimum value for  $[\text{H}\cdot]$  is chosen, the  $[\text{NO}_2]$  present in the experiment can be obtained by subtracting  $[\text{H}\cdot]$  from the initial  $[\text{NO}_2]$ . Applying this method to the data of Table 7, we calculate  $k_{50}/k_{49} = (4 \pm 2) \times 10^3$ , where the uncertainty is caused primarily by inaccuracies in estimating  $[\text{NO}_2]$ .

On the basis of the product distributions and relative rate constants discussed above, we can assess the implications of the OH-aromatic reactions with respect to the environment. As was stated initially, the two major pathways for the reaction are hydrogen atom abstraction, reaction 40 and ring-addition, reaction 41. The fate of the benzylic radical formed in reaction 40 will be governed by reactions 43, 44, and 46, and aromatic aldehyde will be the sole product. This judgment is based on the rate constants for the analogous reactions of methyl,<sup>79</sup> methylperoxy,<sup>80,81</sup> and methoxy<sup>82,83</sup> radicals, and the typical value of  $[\text{O}_2]/[\text{NO}_2] \sim 10^6$  under ambient conditions. The ambient  $[\text{O}_2]/[\text{NO}_2]$  ratio also plays an important role in establishing the ultimate products from reaction 41 because the adduct I is partitioned between reaction 49, with  $\text{O}_2$ , to give phenolic products and reaction 50, with  $\text{NO}_2$ , to give nitroaromatics. Using equation 55 and our values of  $k_{40}/(k_{40} + k_{41}) = 0.15$  and  $k_{50}/k_{49} = 4 \times 10^3$  for toluene, we have calculated the yield of  $3\text{-NO}_2\text{C}_6\text{H}_4\text{CH}_3$  expected for various concentrations of  $\text{NO}_2$ .

$$3\text{-NO}_2\text{C}_6\text{H}_4\text{CH}_3/(\text{total products}) = \{1 - [k_{40}/k_{40} + k_{41}]\}(k_{11}/k_{10})([\text{NO}_2]/[\text{O}_2]) \quad (57)$$

These values are given in Table 11. The table shows that  $3\text{-NO}_2\text{C}_6\text{H}_4\text{CH}_3$  can be a major product for artificially high concentrations of  $\text{NO}_2$ , but that under typical ambient concentrations of  $\text{NO}_2$  (i.e.,  $< 1$  ppm), the yield of nitrotoluene will be less than 1 percent of the total products. Thus we predict that in the environment, reaction 41 will lead exclusively to phenolic products. Table 12 summarizes the atmospheric product distributions expected from the reaction of OH with various aromatic hydrocarbons. In all cases, aromatic aldehydes and

phenols are the predicted products. Because these species have not been reported as constituents of polluted urban atmospheres, it seems likely that they are rapidly removed by as yet undetermined secondary reactions.

A final point concerns recent smog chamber experiments<sup>97,98</sup> with toluene, in which 2-, 3-, and 4-nitrotoluene and isomeric nitrocresols are found as products in addition to the expected benzaldehyde and cresols. The appearance of nitrotoluenes is readily accounted for by the elevated ( $\approx 1$  ppm and greater) concentrations of  $\text{NO}_2$  and high conversions used in the experiments. That the 2- and 4-isomers of nitrotoluene are observed is perplexing, because we have shown that the OH attack on the meta- to the methyl group (the reaction that would lead to the 2- and 4-nitrotoluenes) is of minor importance. Because ionic nitrations typically give predominately 2- and 4-substitution, and because we find<sup>69</sup>  $\text{NO}_x$  to be a powerful nitrating agent in condensing our reaction mixtures, we suggest that the observance of 2- and 4-nitrotoluenes in smog chamber studies is indicative of heterogeneous reactions that occur in the aerosol phase or during sampling of the products. Phenolic compounds are especially susceptible to heterogeneous nitration, and the origin of nitrophenols in smog chamber experiments must be interpreted with extreme caution.

Table 11. CALCULATED<sup>a</sup> YIELD OF 3-NITROTOLUENE (3-NO<sub>2</sub>C<sub>6</sub>H<sub>4</sub>CH<sub>3</sub>/TOTAL PRODUCTS) FROM OH-TOLUENE REACTION AS A FUNCTION OF NO<sub>2</sub> CONCENTRATION<sup>b</sup>

$10^{-13}$	$\frac{[\text{NO}_2]}{\text{cm}^3 \text{ mole}^{-1}}$	ppm	$\frac{3\text{-NO}_2\text{C}_6\text{H}_4\text{CH}_3}{(\text{total products})}$
	1.10	0.04	$5.4 \times 10^{-4}$
	3.0	0.12	$1.63 \times 10^{-3}$
	10.0	0.40	$5.4 \times 10^{-3}$
	30.0	1.2	$1.6 \times 10^{-2}$
	100.0	4.0	$5.4 \times 10^{-2}$
	300.0	12.0	$1.6 \times 10^{-1}$

<sup>a</sup>Calculated from equation 57.

<sup>b</sup>[O<sub>2</sub>] = 0.21 atm.

Table 12. ATMOSPHERIC PRODUCTS FOR THE REACTIONS OF AROMATIC HYDROCARBONS WITH OH

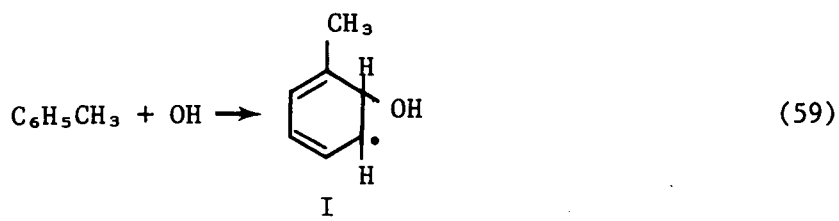
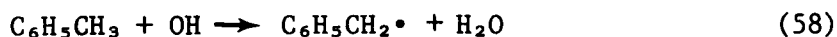
Hydrocarbon	Atmospheric Products <sup>a</sup>
C <sub>6</sub> H <sub>6</sub>	C <sub>6</sub> H <sub>5</sub> OH, 100%
C <sub>6</sub> H <sub>5</sub> CH <sub>3</sub>	C <sub>6</sub> H <sub>5</sub> CHO, 15%
	2-, 3-, 4-HOC <sub>6</sub> H <sub>4</sub> CH <sub>3</sub> , 85%
1,4-(CH <sub>3</sub> ) <sub>2</sub> C <sub>6</sub> H <sub>4</sub>	4-CH <sub>3</sub> C <sub>6</sub> H <sub>4</sub> CHO, 15%
	2,5-(CH <sub>3</sub> ) <sub>2</sub> C <sub>6</sub> H <sub>3</sub> OH, 85%
1,3,5-(CH <sub>3</sub> ) <sub>3</sub> C <sub>6</sub> H <sub>3</sub>	3,5-(CH <sub>3</sub> ) <sub>2</sub> C <sub>6</sub> H <sub>3</sub> CHO, 2%
	2,4,6-(CH <sub>3</sub> ) <sub>3</sub> C <sub>6</sub> H <sub>2</sub> OH, 98%

<sup>a</sup>Assuming [NO<sub>2</sub>] < 1 ppm, O<sub>2</sub> = 2.5 x 10<sup>5</sup> ppm.

## 5. GAS PHASE HYDROXYL RADICAL REACTIONS. PRODUCTS AND PATHWAYS FOR THE REACTION OF OH WITH BENZALDEHYDE

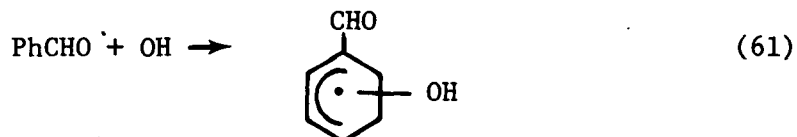
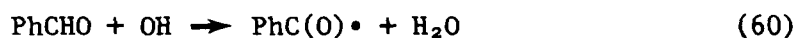
### INTRODUCTION

Single-ring aromatic hydrocarbons comprise a high proportion of the carbon found in polluted urban atmospheres<sup>48,99</sup> and are known<sup>50-53</sup> to produce a variety of adverse effects (eye irritation, ozone, oxidant, and peroxy-nitrate formation, and so forth) associated with photochemical smog. It is therefore important that the atmospheric chemistry of aromatic hydrocarbons be understood in detail. Studies of the kinetics of the gas phase reactions of aromatic hydrocarbons with species such as hydroxyl radical,<sup>53-58</sup> oxygen atom,<sup>100</sup> ozone<sup>101</sup> and peroxy radicals<sup>102</sup> leave little doubt that reaction with OH is by far the most important route for involvement of aromatics in the chemistry of the troposphere. We previously<sup>103</sup> discussed the mechanism of the toluene reaction and demonstrated that the major pathways for the reaction are hydrogen atom abstraction, reaction 58, and addition to the aromatic ring, reaction 59.



In the ambient, reactions 58 and 59 would ultimately lead to benzaldehyde and isomeric cresols, respectively. Because neither benzaldehyde nor cresols are observed to accumulate in the troposphere, it seems likely that these compounds are themselves rapidly transformed. A recent determination<sup>104</sup> of the rate constant for reaction of OH with benzaldehyde ( $k_{\text{PhCHO}} = 1.3 \times 10^{-11} \text{ cm}^3 \text{ molec}^{-1} \text{ s}^{-1}$ ) suggests that this reaction plays an important role in determining the fate of benzaldehyde in the atmosphere.

Accordingly, we have undertaken to elucidate the products and mechanisms of the OH-PhCHO reaction. By analogy with the OH-toluene reaction, abstraction of aldehydic hydrogen (reaction 60), and ring-addition by OH (reaction 61), must both be considered.



In fact, however, we find that reaction 60 proceeds to the exclusion of reaction 61. In the following, we detail our experimental observations and discuss their environmental ramifications.

#### EXPERIMENTAL SECTION

Hydroxyl radicals were generated in a discharge-flow system by reaction 62



The method used has been described in detail elsewhere<sup>70-76,103</sup>. All reactions were carried out at ambient temperature ( $25 \pm 3^\circ\text{C}$ ). Typically,  $2 \times 10^{-2}$  torr  $\text{H}_2$  in 5 torr Ar was passed through a microwave discharge and the hydrogen atoms so produced were reacted with 2 to  $5 \times 10^{-3}$  torr  $\text{NO}_2$ . A mixture of 5 to  $10 \times 10^{-2}$  torr PhCHO in 1 to 5 torr of an  $\text{O}_2$  plus Ar mixture was admitted 5 cm downstream from the point of addition of  $\text{NO}_2$ . With a linear velocity of  $1 \times 10^3$  cm-sec<sup>-1</sup>, reaction 62 ( $k_{62} = 4.8 \times 10^{-11}$  cm<sup>3</sup>-molec<sup>-1</sup> s<sup>-1</sup>)<sup>78</sup> has gone to completion at this point. Because the amount of PhCHO added was large compared to the hydroxyl radical concentrations attained ( $[\text{OH}] \sim 5 \times 10^{-4}$  torr<sup>77</sup>), conversions were low and secondary reactions were minimized. Gas phase products were trapped on a solid adsorbent (Tenax-GC)<sup>105,106</sup> and then analyzed by glpc. In addition to gas phase products, a significant amount of solid residue accumulated on the



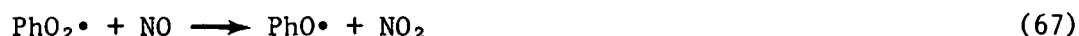
walls of the flow system. This residue was physically removed from the walls, weighed, and subjected to elemental analysis. Then it was analyzed by field ionization mass spectral (FIMS) which gives exclusively the parent peaks in proportion to the composition of the components.

## RESULTS

In all reactions studied, the only observable gas phase product was phenol (PhOH). Benzoic acid, perbenzoic acid, peroxybenzoyl nitrate, and 2- and 3-hydroxybenzaldehyde were looked for but not found. The yield of PhOH (expressed as a percent of PhCHO) was determined under conditions of varying NO<sub>2</sub>, O<sub>2</sub>, and total pressure. These results are summarized in Table 13.

In Table 14, some characteristics of the wall residue and the gas phase product are presented. Finally, mass spectral data for the wall residue are present in Table 15.

In Table 13, we see that the yield of PhOH is on the order of 1 to 2% (consistent with the low conversions expected) for a variety of [NO<sub>2</sub>] and O<sub>2</sub> pressures (runs 1-7). However, for runs 8-11, in which O<sub>2</sub> was eliminated from the reaction system, the yield of PhOH decreases by an order of magnitude. These data indicate the PhOH is formed by reactions 60 and 63-68.



This mechanism satisfactorily explains the observed oxygen dependence of the PhOH yield. An alternative mechanism involving ipso-attack by

Table 13. PERCENT YIELD OF PHENOL ( $100 \times \text{PhOH}/\text{PhCHO}$ ) AS A  
FUNCTION OF ADDED  $\text{NO}_2$ ,  $\text{O}_2$  AND TOTAL PRESSURE

Run	$\text{NO}_2$ torr $\times 10^3$	$\text{O}_2$ torr	Total Pressure Ar + $\text{O}_2$ torr	$\frac{100 \times \text{PhOH}}{\text{PhCHO}}$
1	1.08	4	10	2.11
2	2.70	4	10	2.21
3	4.05	4	10	2.19
4	5.40	21	10	1.22
5	2.70	4	10	1.89
6	2.70	3	10	1.85
7	2.70	1	10	1.48
8	1.08	0	6	0.091
9	2.70	0	6	0.095
10	4.05	0	6	0.084
11	5.40	0	6	0.019

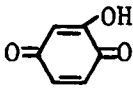
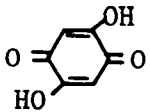
Table 14. WALL AND GAS PHASE PRODUCTS OF THE OH-PhCHO REACTION AS A FUNCTION OF ADDED NO<sub>2</sub><sup>a</sup>

Run	NO <sub>2</sub>	$\frac{100 \times \text{PhOH}}{\text{PhCHO}}$	Total PhOH <sup>b</sup>	Wall Residue	Wall Analysis, %			
	torr x 10 <sup>3</sup>		gm	gm	C	H	N	O
12	1.35	2.15	0.31	0.16	49.2	4.74	0.42	45.6
13	3.24	2.0	0.35	0.079	49.4	4.62	1.49	44.5

<sup>a</sup> O<sub>2</sub> = 4 torr, total pressure 10 torr.

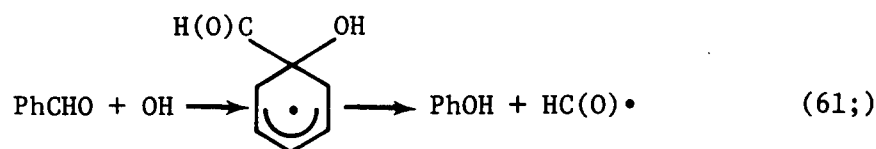
<sup>b</sup> Total PhOH = (PhOH/PhCHO) • (total moles PhCHO added) • (94 gm/mole).

Table 15. FIELD IONIZATION MASS SPECTRAL ANALYSIS OF WALL RESIDUE FOR  
OH-PhCHO REACTION<sup>a</sup>

m/e	Rel Ht	% of Total	Formula	Possible Structure
94	7.5	2.5	C <sub>6</sub> H <sub>6</sub> O	PhOH
110	70.4	23.0	C <sub>6</sub> H <sub>6</sub> O <sub>2</sub>	Ph(OH) <sub>2</sub>
122	4.4	1.5	C <sub>7</sub> H <sub>6</sub> O <sub>2</sub>	PhC(O)OH or HOPhCHO
124	100	33.0	C <sub>6</sub> H <sub>4</sub> O <sub>3</sub>	
126	14.5	4.8	C <sub>6</sub> H <sub>6</sub> O <sub>3</sub>	Ph(OH) <sub>3</sub>
138	10.1	3.4	C <sub>7</sub> H <sub>6</sub> O <sub>3</sub>	HOPhC(O)OH or (HO) <sub>2</sub> PhCHO
139	24.5	8.1	C <sub>6</sub> H <sub>5</sub> NO <sub>3</sub>	HOPhNO <sub>2</sub>
140	10.1	3.4	C <sub>6</sub> H <sub>4</sub> O <sub>4</sub>	Ph(OH) <sub>4</sub>
152	5.0	1.7	C <sub>7</sub> H <sub>4</sub> O <sub>4</sub>	
154	12.6	4.2	C <sub>7</sub> H <sub>6</sub> O <sub>4</sub>	(HO) <sub>2</sub> PhC(O)OH or (HO) <sub>4</sub> PhCHO
155	8.2	2.7	C <sub>6</sub> H <sub>5</sub> NO <sub>4</sub>	(HO) <sub>2</sub> PhNO <sub>2</sub>
168	7.5	2.5	C <sub>6</sub> H <sub>4</sub> N <sub>2</sub> O <sub>4</sub>	Ph(NO <sub>2</sub> ) <sub>2</sub>
170	4.4	1.5	C <sub>12</sub> H <sub>10</sub> O	Ph-PhOH
186	16.0	5.3	C <sub>12</sub> H <sub>10</sub> O <sub>2</sub>	HOPh-PhOH
202	6.3	2.1	C <sub>12</sub> H <sub>10</sub> O <sub>3</sub>	PhPh(OH) <sub>3</sub>

<sup>a</sup>Residue of Run 12, see Table 14.

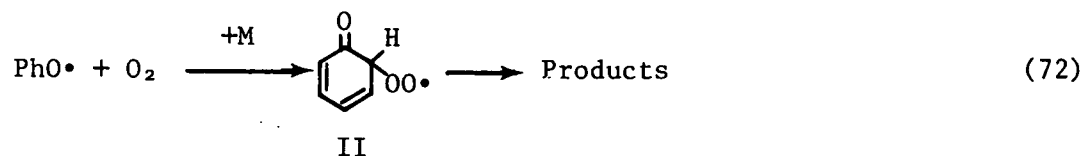
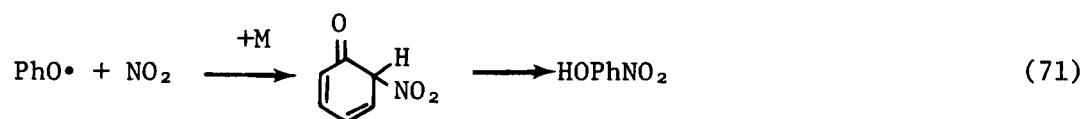
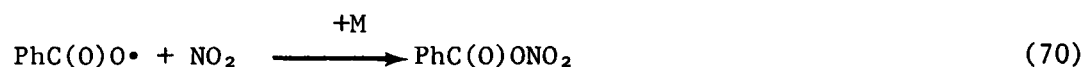
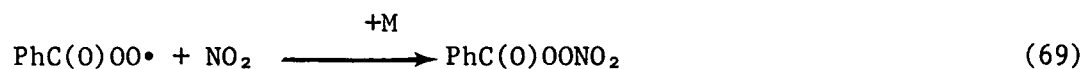
hydroxyl radical (reaction 61;)



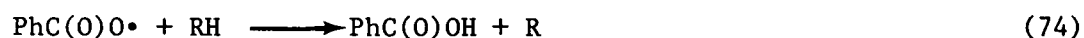
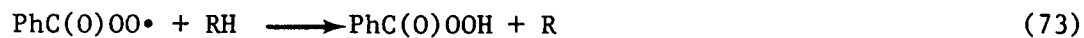
is rejected on the grounds that the yield of phenol in this case would be independent of the concentration of added oxygen.

The absence of gas phase products other than PhOH can be explained by suggesting that such products might be formed only by reactions that would be conceivable under other conditions, but that are prohibitively slow under the low total pressures and reactant concentrations used in our system.

For example, reactions 69-72 are unlikely in our system because of the low total pressures employed.



Similarly, the hydrogen atom abstraction reactions 73 - 75 are slow as a result of low radical and hydrogen atom donor concentrations.



As an example, for  $\text{RH} = \text{PhCHO}$  at  $5 \times 10^{-2}$  torr ( $1.6 \times 10^{15}$  molec  $\text{cm}^{-3}$ ), the half-life for disappearance of  $\text{PhC(O)OO}\cdot$  by reaction 73 is approximately 20 s ( $k_{73} = 2 \times 10^{-17}$   $\text{cm}^3$  molec $^{-1}$  s $^{-1}$ ).<sup>107</sup> At the same time, for  $\text{NO} = 5 \times 10^{-3}$  torr, the half-life for  $\text{PhC(O)OO}\cdot$  disappearance by reaction 64 is  $10^{-3}$  s, assuming  $k_{64} = 3 \times 10^{-12}$   $\text{cm}^3$  molec $^{-1}$  s $^{-1}$  (i.e., assuming  $k_{64}$  equals the rate constant for reaction of  $\text{CH}_3\text{C(O)OO}\cdot$  plus  $\text{NO}$ <sup>108</sup>).

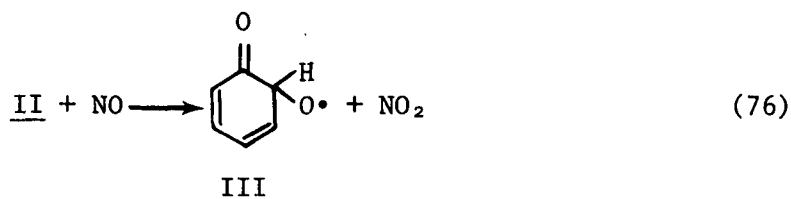
## DISCUSSION

Because no facile gas phase reactions are available to  $\text{PhO}\cdot$ , it is primarily consumed by heterogeneous processes at the reactor walls. The extent of wall reactions in the  $\text{OH-PhCHO}$  system is demonstrated by the data of Table 14. In run 12, for example, the total yield of  $\text{PhOH}$  was 0.31 gm, and a total of 0.16 gm of wall residue was recovered. Interestingly, the majority of the wall products are  $\text{C}_6$  or  $\text{C}_{12}$  species, i.e., species derived ultimately from reactions 60 and 63-68, the only possible exceptions being compounds with  $m/e = 122, 138, 152, \text{ and } 154$ . Because these species constitute only 10% of the wall product, which in turn amounts to only about one-third of the total gas phase plus wall product, we set 3% as the upper limit for addition of  $\text{OH}$  to  $\text{PhCHO}$  through reaction 61.

The preponderance of abstraction over addition in the  $\text{OH-PhCHO}$  reaction is a dramatic reversal of the trend observed for reaction of  $\text{OH}$  with methyl-substituted benzenes. In these reactions,<sup>103</sup> ring-addition was the preferred process, constituting 85 to 98% of the total reaction for the substrates investigated. This difference is rationalized on the basis of the electrophilic nature of the hydroxyl radical. Both studies reported in the previous section and kinetic studies<sup>58</sup> show that ring-addition by  $\text{OH}$  is enhanced by electron-donating substituents. We expect, therefore, that the formyl group (an electron withdrawing substituents) should slow the rate of reaction 59 relative to the rate of addition of  $\text{OH}$  to benzene. Even using the  $\text{OH-benzene}$  rate constant,  $k_{\text{PhH}} = 1.2 \times 10^{-12}$   $\text{cm}^3$  molec $^{-1}$  s $^{-1}$ ,<sup>58</sup> as an upper limit for the rate of reaction 61, the overall rate constant for  $\text{OH}$  plus benzaldehyde,  $k_{\text{PhCHO}} = 1.3 \times 10^{-11}$   $\text{cm}^3$  molec $^{-1}$  s $^{-1}$ ,<sup>104</sup> is sufficiently fast that ring-addition by  $\text{OH}$  to  $\text{PhCHO}$  can be only

a minor fraction of the total reaction pathway.

Since it has been demonstrated that the OH-PhCHO reaction proceeds virtually entirely through reaction 60 as the initial step, it remains to identify the products of the reaction under atmospheric conditions. Formation of peroxybenzoyl nitrate by reaction 69 is likely under conditions where  $\text{NO}_2/\text{NO}$  is high. As with peroxyacetyl nitrate,<sup>108</sup> however, the peroxybenzoyl nitrate should be in equilibrium with  $\text{PhC(O)OO}\cdot$  and  $\text{NO}_2$ , i.e., reaction 69 should be reversible. Because of this, peroxybenzoyl nitrate acts as a reservoir of benzoylperoxy radicals, and the latter will be consumed in reaction 64 when the ambient concentration of NO is high. Benzoyloxy radicals formed in reaction 64 are expected to yield phenoxy radical through reactions 65-67. As a consequence, the fate of PhCHO in the environment will be largely governed by the fate of the phenoxy radical. Although we cannot specify the fate of  $\text{PhO}\cdot$  with certainty, it seems likely that it would react at atmospheric pressure primarily through reactions 71 and 72, which lead to ring cleavage. Reaction 71 gives isomeric nitrophenols as the stable products. Emphasizing the importance of reaction 71 is the recent observation of nitrophenols as products from  $\text{PhC(O)}\cdot$  plus  $\text{O}_2$  plus  $\text{NO}_x$  in the chlorine atom initiated oxidation of PhCHO.<sup>109</sup> As to reaction 72, it is likely to be reversible even at atmospheric pressure, owing to the weak C-O<sub>2</sub> bond strength in the intermediate II. We estimate  $\text{DH}^\circ(\text{C-O}_2) = 10 \text{ kcal/mole}$ . To the extent to which reaction 72 is not reversible, the adduct II will react with NO as in reaction 76.



Suggestions for subsequent reactions of III are speculative, but oxidative ring-opening to yield low-molecular-weight carbonyl compounds is a possibility.

An important distinction to be made is that reaction 71 terminates radical chains and removes  $\text{NO}_2$  from the atmosphere, whereas reactions 72 and 76 propagate radical chains and affect the important oxidation of  $\text{NO}$  to  $\text{NO}_2$ .

The partitioning of phenoxy radical between reactions 71 and 72 therefore plays a potentially important role in the formation of photochemical smog. For this reason, further studies on the atmospheric reactions of  $\text{PhO}\cdot$  would be of interest.



## REFERENCES AND NOTES

1. J. N. Pitts and B. J. Finlayson, Angew. Chem. (Int. Ed.), 14, 1 (1975).
2. J. A. Kerr, J. G. Calvert, and K. L. Demerjian, Chem. Brit., 8, 252 (1970).
3. E. R. Stephens, in "Advances in Environmental Sciences," Vol. I, J. N. Pitts and R. L. Metalf, Eds. (Wiley-Interscience, New York, 1969) p. 119.
4. E. F. Darley, K. A. Kettner, and E. A. Stephens, Anal. Chem., 35 589 (1963).
5. H. Mayrsohn and C. Brooks, presented at Western Regional Meeting of the American Chemical Society, (1965).
6. O. C. Taylor, J. Air Poll. Cont. Assoc., 19 (5), 347 (1969).
7. D. T. Tingey and A. C. Hill, Utah Acad. Proc., 44 (1), 387 (1967).
8. "Air Quality Criteria for Photochemical Oxidants" Nat. Air Poll. Cont. Assoc. Admin. Publc. Ap-63, pp 3-10 (1970).
9. W. A. Lonnemann, J. J. Bufalini, and R. L. Seila, Environ. Sci. Tech., 10 (4), 374 (1976).
10. S. A. Penkett, F. J. Sandalls, and J. E. Lovelock, Atmos. Environ., 9 139 (1975).
11. H. Nieboer and J. vanHam, TNO Nieuws, 5, 170 (1972).
12. H. Nieboer and J. vanHam, Atmos. Environ., 10 (7), 115 (1976).
13. E. R. Stephens, E. F. Darley, O. C. Taylor, and W. E. Scott, Int. J. Air Water Poll., 4 (1,2), 79 (1961); Proc. Am. Petrol. Inst. Sec. III, 40 325 (1960).
14. E. F. Darley, C. W. Nichols, and J. T. Middleton, Calif. Dept. Agr. Bull, 55 (11) 1966.
15. E. F. Darley, W. M. Dugger, J. B. Mudd, L. Ordin, O. C. Taylor, and E. R. Stephens, Arch. Environ. Health, 6 761 (1963).

16. D. G. Hendry and R. A. Kenley, J. Am. Chem. Soc., 99, 3198 (1977).
17. D. Swern, in "Organic Peroxides," Vol. I, D. Swern, Ed. (Wiley-Interscience, New York, 1970, p. 480).
18. R. Louw, G. J. Sluis, and H.P.W. Vermoren, J. Am. Chem. Soc., 97 (15), 4396 (1975).
19. E. R. Stephens, F. R. Burleson, and E. A. Cardiff, J. Air Poll. Cont. Assoc., 15 (3), 87 (1965).
20. P. Gray and A. D. Yoffe, Chem. Rev., 55, 1069 (1955).
21. E. R. Stephens, F. R. Burleson, and K. M. Holtzclaw, J. Air Poll. Cont. Assoc., 19 (4) 261 (1969).
22. W. J. Braun, L. Rajenbach, and F. R. Eirich, J. Phys. Chem., 66, 1959 (1962).
23. K. U. Ingold, in "Free Radicals," Vol. I, J. K. Kochi, Ed. (Wiley-Interscience, New York, 1973 p. 1.)
24. S. W. Benson, "Thermochemical Kinetics — Methods for the Estimation of Thermochemical Data and Rate Parameters" (J. Wiley and Sons, New York, 1968).
25. L. J. Bellamy, "The Infrared Spectra of Complex Molecules," (Wiley-New York, 1958).
26. K. Nakamoto, "Infrared Spectra of Inorganic and Coordination Compounds," (Wiley-Interscience, New York, 1963, p. 94).
27. E. R. Allen, and K. W. Bagley, Berg. Bunsengesell., 72, 227 (1968).
28. A. E. Pedler and F. H. Pollard, Trans. Far. Soc., 53, 44 (195 ).
29. L. Phillips and R. Shaw, 10th Smp. (Int.) on Combust., 453 (1961).
30. J. A. Howard, in "Free Radicals," Vol. II; J. K. Kochi, Ed. (Wiley-Interscience, New York, 1977, p. 1).
31. J. A. Howard in "Advances in Free Radical Chemistry," Vol. IV, G. A. Williams, Ed. (Academic Press, New York, 1972).
32. F. A. Cotton and G. Wilkinson, Advanced Inorganic Chemistry, 2nd Edition (Wiley, New York, 1966) p. 355.
33. D. Gray, E. Lissi, and J. Heicklen, J. Phys. Chem., 76, 1919 (1972).
34. E. L. Varette and G. C. Pimentel, Spectrochim. Acta, 30A, 1069 (1974).

35. E. T. Arakawa and A. H. Nielsen, J. Mol. Spectry, **2**, 413 (1958).
36. C. T. Pate, R. Atkinson, and J. N. Pitts, Environ. Sci. Eng., **A11**, 19 (1976). These authors report  $k_{-1} = 2.8 (\pm 0.8) \times 10^{-4} \text{ s}^{-1}$  at  $23 \pm 1^\circ \text{C}$  using PAN and NO in much lower concentrations (PAN  $\approx 10^{-7} \text{ M}$ , NO  $\sim 10^{-6} \text{ M}$ ).
37. Stephens and co-workers (see references 3 and 13) originally proposed a six-center cyclic elimination of  $\text{CH}_3\text{ONO}_2$  and  $\text{CO}_2$  as the mechanism for the decomposition of PAN. As with reaction 6, the rate for the cyclic elimination can be no faster than the decomposition of pure PAN in the absence of added reactants.
38. E. S. Domalski, Environ. Sci. and Technology, **5**, 443 (1971).
39. S. W. Benson, F. R. Cruickshank, D. M. Golden, G. R. Haugen, H. E. O'Neal, A. S. Rogers, R. Shaw, and R. Walsh, Chem. Rev., **69**, 279 (1969).
40. S. W. Benson and R. Shaw, in "Organic Peroxides," D. Swern, Ed., (Wiley-Interscience 1970, p. 105).
41. "JANAF Thermochemical Tables," 2nd Edition, U.S. Department of Commerce, National Bureau of Standards, NSRDS-NBS 37, Washington, D.C., (1971).
42. S. W. Benson and H. E. O'Neal, "Kinetic Data on Gas Phase Unimolecular Reactions," U.S. Department of Commerce, National Bureau of Standards, NSRDS-NBS 21, Washington, D.C. (1970).
43. C. J. Howard and K. M. Evenson, Trans. Amer. Geophys. Union, **58**, 464 (1977).
44. D. G. Hendry, unpublished results.
45. E.F.J. Duynstee, J.L.J.D. Hennekens, J.G.H.M. Hausmans, W. Van Raayen, and W. Voskuil, Rec. Trav. Chem. Pays-Bas, **92**, 1272 (1973).
46. E. M. Kuramshin and V. D. Komissarov, Izv. Akad. Navk. SSSR, Ser. Khim, 1937 (1976).
47. R. A. Cox and M. J. Roffey, Enviro. Sci. Tech., **11**, 900 (1977).
48. W. A. Lonneman, S. L. Kopczinski, P. E. Darley, and F. D. Sutterfield, Environ. Sci. Tech., **8**, 229 (1974).
49. J. M. Heuss and W. A. Glasson, Environ. Sci. Technol., **2**, 1109 (1968).
50. A. P. Altshuller, S. L. Kopczinski, D. Wilson, W. Lonneman, and F. D. Sutterfield, J. Air Poll. Contr. Assoc., **19**, 291 (1969).

51. A. P. Altschuller, S. L. Kopczinski, W. A. Lonneman, F. D. Sutterfield, and D. L. Wilson, Environ. Sci. Technol., 4, 44 (1970).
52. J. M. Heuss, G. J. Nebel, and B. A. D'Alleva, Environ. Sci. Technol., 8, 641 (1974).
53. F. D. Morris and H. Niki, J. Phys. Chem., 75, 3641 (1971).
54. D. A. Hansen, R. Atkinson, and J. N. Pitts, J. Phys. Chem., 79, 1763 (1975).
55. D. D. Davis, W. Bollinger, S. Fischer, J. Phys. Chem., 79, 293 (1975).
56. G. J. Doyle, A. C. Lloyd, K. R. Darnall, A. M. Winer, and J. N. Pitts, Environ. Sci. Technol., 9, 237 (1975).
57. A. C. Lloyd, K. R. Darnall, A. M. Winer, and J. N. Pitts, J. Phys. Chem., 80, 789 (1976).
58. R. A. Perry, R. Atkinson, and J. N. Pitts, J. Phys. Chem., 81, 296 (1977).
59. K. R. Darnall, A. C. Lloyd, A. M. Winer, and J. N. Pitts, Environ. Sci. Technol., 10, 692 (1976).
60. K. R. Darnall, G. J. Doyle, A. M. Winer, and J. N. Pitts, Environ. Sci. Technol., 12, 100 (1978).
61. L. M. Dorfman, I. A. Traub, and D. A. Harter, J. Chem. Phys., 41, 2954 (1964).
62. K. Sehested, H. Corfitzen, H. C. Christensen, and E. J. Hart, J. Phys. Chem., 79, 310 (1975).
63. H. C. Christensen, K. Sehested, and E. J. Hart, J. Phys. Chem., 77, 983 (1973).
64. M. Anbar, D. Meyerstein, and P. Neta, J. Phys. Chem., 70, 2660 (1966).
65. J.R.L. Smith and R.O.C. Norman, J. Chem. Soc., 1963, 2897 (1963).
66. C.R.E. Jefcoate, J.R.L. Smith, and R.O.C. Norman, J. Chem. Soc. (B), 1969, 1013 (1969).
67. R. Tomat and A. Rigo, J. Appl. Electrochem., 6, 257 (1976).
68. Y. Ogata and K. Tomizawa, J. Org. Chem., 43, 261 (1978).

69. In some instances products indicative of ionic (as opposed to free radical) reactions were found in the cold traps. In general, these side reactions could be eliminated by sampling at  $-78^{\circ}\text{C}$  rather than  $-196^{\circ}\text{C}$  and by working at low pressures ( $\leq 5 \times 10^{-3}$  torr) of added  $\text{NO}_2$ .
70. F. Kaufman and F. P. Del Greco, J. Chem. Phys., **35**, 1895 (1961).
71. F. P. Del Greco and F. Kaufman, Disc. Far. Soc., **33**, 128 (1962).
72. L. F. Phillips and H. I. Schiff, J. Chem. Phys., **37**, 1233 (1962).
73. J. E. Breen and G. P. Glass, Int. J. Chem. Kin., **3**, 145 (1970).
74. J. E. Breen and G. P. Glass, J. Chem. Phys., **52**, 1082 (1972).
75. A. Pastrana and R. W. Carr, Int. J. Chem. Kin., **6**, 587 (1974).
76. W. E. Wilson, J. Phys. Chem. Ref. Data, **1**, 535 (1972).
77. Concentrations estimated from a detailed chemical model of the reaction system; see text.
78. CIAP Monograph 1, DOT-TST-75-51, page 5-232 (1975).
79. D. A. Parkes, Int. J. Chem. Kin., **9**, 451 (1977).
80. R. Simonaitis and J. Heicklen, J. Phys. Chem., **78**, 2417 (1974).
81. C. T. Pate, B. J. Finlayson, and J. N. Pitts, J. Amer. Chem. Soc., **96**, 6554 (1974).
82. J. R. Barker, S. W. Benson, and D. M. Golden, Int. J. Chem. Kin., **9**, 31 (1977).
83. L. Batt, R. T. Milne, and R. D. McCulloch, Int. J. Chem. Kin., **9**, 567 (1977).
84. D. G. Hendry and D. Schuetzle, J. Amer. Chem. Soc., **97**, 7123 (1975).
85. E. Halfpenny and P. L. Robinson, J. Chem. Soc., 939 (1952).
86. T. Suehiro, M. Hirai, and T. Kaneko, Bull. Chem. Soc. Jap., **44**, 1407 (1971).
87. M. E. Kurz, R. L. Fozdar, and S. S. Schultz, J. Org. Chem., **39**, 3336 (1974).
88. R. Simonaitis and J. Heicklen, J. Phys. Chem., **78**, 653 (1974).

89. R. Simonaitis and J. Heicklen, J. Phys. Chem., 80, 1 (1976).
90. C. J. Howard and K. M. Evenson, Trans. Am. Geophys. Union, 58, 464 (1977).
91. R. A. Graham, A. M. Winer, and J. N. Pitts, Chem. Phys. Lett., 51, 215 (1977).
92. E. Grovenstein and A. J. Mosher, J. Am. Chem. Soc., 92, 3810 (1970).
93. I. Mani and M. C. Sauer, Adv. Chem. Ser., 82, 142 (1968).
94. G. A. Olah, Accts. Chem. Res., 4, 240 (1971).
95. J. C. Martin, in Free Radicals, Vol. II, J. Kochi, ed., p. 516, (Wiley-Interscience, New York, 1973).
96. R.O.C. Norman and G. K. Radda, Proc. Chem. Soc. 1962, 138 (1962).
97. R. J. O'Brien, P. J. Green, and R. A. Doty, "Interaction of Oxides of Nitrogen with Aromatic Hydrocarbons," 175th National Meeting of the American Chemical Society, March 1978.
98. D. R. Fitz, D. Grosjean, K. Van Cauwenbergher, and J. N. Pitts, "Photooxidation Products of Toluene-NO<sub>x</sub> Mixtures Under Simulated Atmospheric Conditions," *ibid.*
99. J. G. Calvert, Environ. Sci. Tech., 10, 256 (1976).
100. R. Atkinson and J. N. Pitts, J. Phys. Chem., 79, 295 (1975).
101. T. W. Nakagawa, L. J. Andrews, and R. M. Keefer, J. Am. Chem. Soc., 82, 269 (1960).
102. D. G. Hendry, T. Mill, L. Piszkiwicz, J. A. Howard, and H. K. Eigenmann, J. Phys. Chem. Ref. Data, 3, 937 (1974).
103. R. A. Kenley, J. E. Davenport, D. G. Hendry, J. Phys. Chem., 82, 1095 (1978).
104. H. Niki, P. D. Maker, C. M. Savage, and L. P. Breitenbach, J. Phys. Chem., 82, 132 (1978).
105. E. D. Pellizari, J. E. Bunch, and B. H. Carpenter, Environ. Sci. Tech., 9, 552 (1975).
106. E. D. Pellizari, B. H. Carpenter, and J. E. Bunch, Environ. Sci. Tech., 9, 556 (1975).

- 107 J. A. Howard, in Advances in Free-Radical Chemistry, Vol. IV, p. 99 (Academic, New York, 1972).
- 108. R. A. Kenley and D. G. Hendry, J. Am. Chem. Soc., 99, 3198 (1977).
- 109. H. Niki, P. F. Maker, C. M. Savage, and L. P. Breitenbach, "Fourier Transform IR Studies of Gaseous and Particulate Nitrogenous Compounds of Atmospheric Interest," 175th National Meeting of the American Chemical Society, March 1978.

TECHNICAL REPORT DATA (Please read Instructions on the reverse before completing)		
1. REPORT NO. EPA -600/3-79-020	2.	3. RECIPIENT'S ACCESSION NO.
4. TITLE AND SUBTITLE REACTIONS OF OXY RADICALS IN THE ATMOSPHERE	5. REPORT DATE March 1979	6. PERFORMING ORGANIZATION CODE
	8. PERFORMING ORGANIZATION REPORT NO.	
7. AUTHOR(S) D.G. Hendry, R.A. Kenley, J.E. Davenport, and B.Y. Lan	10. PROGRAM ELEMENT NO. 1AA603 AC-21 (FY-78)	
9. PERFORMING ORGANIZATION NAME AND ADDRESS SRI International 333 Ravenswood Ave. Menlo Park, California 94025	11. CONTRACT/GRANT NO. Grant No. 603864	
	13. TYPE OF REPORT AND PERIOD COVERED Final 6/75 - 6/78	
12. SPONSORING AGENCY NAME AND ADDRESS Environmental Sciences Research Laboratory-RTP, NC Office of Research and Development U.S. Environmental Protection Agency Research Triangle Park, North Carolina 27711	14. SPONSORING AGENCY CODE EPA/600/09	
	15. SUPPLEMENTARY NOTES	
16. ABSTRACT <p>Results are presented of a research program concerned with the study of selected reactions of importance in atmospheric chemistry. The decomposition of peroxyacetyl nitrate (PAN) was studied over the temperature range 25-39°C. The rate constant was determined to be <math>\log k = 16.29 - 26,910/4.576 T</math>. The reactions of acetylperoxy radicals with NO and NO<sub>2</sub> were investigated. The ratio of the rate constants for these reactions was determined to be <math>k_{NO}/k_{NO_2} = 3.0 \pm 0.7</math>.</p> <p>The products of the reaction of OH with various aromatic compounds were also determined. The investigation showed that the reaction of OH with simple aromatic hydrocarbons proceeds by two major pathways, abstraction of a hydrogen atom in the benzylic position or addition of OH to the aromatic ring. Ratios of the rate of abstraction versus addition were determined for toluene, 1,4-dimethylbenzene and 1,3,5-trimethylbenzene.</p> <p>Results of a study to elucidate the products and mechanism of the reaction of OH with benzaldehyde are also presented. Research showed that this reaction proceeds exclusively by abstraction of the aldehydic hydrogen.</p>		
17. KEY WORDS AND DOCUMENT ANALYSIS		
a. DESCRIPTORS	b. IDENTIFIERS/OPEN ENDED TERMS	c. COSATI Field/Group
<ul style="list-style-type: none"> <li>* Air pollution</li> <li>* Photochemical reactions</li> <li>* Reaction kinetics</li> <li>* Oxidation</li> <li>* Aromatic hydrocarbons</li> <li>* Peroxy organic compounds</li> </ul>		13B 07E 07D 07B 07C
18. DISTRIBUTION STATEMENT RELEASE TO PUBLIC	19. SECURITY CLASS (This Report) UNCLASSIFIED	21. NO. OF PAGES 78
	20. SECURITY CLASS (This page) UNCLASSIFIED	22. PRICE